

Martin Widding

QUANTIFYING THE CAPACITY VALUE OF WIND POWER IN COMPOSITE POWER SYSTEMS

Masteroppgave i Energi og Miljø

Veileder: Vijay Vadlamudi

August 2022

Martin Widding

QUANTIFYING THE CAPACITY VALUE OF WIND POWER IN COMPOSITE POWER SYSTEMS

Masteroppgave i Energi og Miljø
Veileder: Vijay Vadlamudi
August 2022

Norges teknisk-naturvitenskapelige universitet
Fakultet for informasjonsteknologi og elektroteknikk
Institutt for elkraftteknikk



Kunnskap for en bedre verden

Abstract

Renewable power is a growing resource, and is an important factor in the future of power system planning. The last decade, wind power and solar photovoltaic power has been the largest growing renewable energy source on the market. However, both wind and solar power are intermittent power sources, and are not possible to schedule in contrast to hydro power and power produced by burning fossil fuels. To accurately value the contribution renewable energy sources have on the power system, a method of quantifying their integration into an existing power system is needed.

This thesis presents and explains a method to quantify the Capacity Value (CV) of wind power generation integrated in an existing composite power system. It is intended as an addition to the ongoing Power System Reliability project at the Department of Electrical Power Engineering at NTNU. The power system's probabilistic nature is simulated through the State Sampling Monte Carlo Simulation method, and the CV metric Effective Load Carrying Capability (ELCC) is determined using the bisection method.

An in-house software tool capable of quantifying the ELCC of added wind power generation to an existing composite power system is developed through this thesis work. The tool is able to base the ELCC calculations on two adequacy reliability indices, namely the Loss of Load Expectation (LOLE) and the Expected Energy not Served (EENS). Using two different indices to calculate the ELCC of added generation to a composite power system is shown to present different perspectives on potential power system expansion.

Through a literature review, the thesis presents a comprehensive explanation of Power System Reliability studies. Both sequential and non-sequential Monte Carlo Simulation methods are explained in detail. The State Sampling method is used in the software developed through this thesis work, as it is found to need fewer simulation years to converge on a result compared to the State Duration and State Transmission methods.

Sammendrag

Fornybar kraft er en voksende ressurs, og er en viktig faktor for fremtiden av kraftsystemplanlegging. Det siste tiåret har vindkraft og solcelleanlegg vært den raskeste voksende energiressursen på markedet. Både vindkraft og solcelleanlegg er intermitterende kraftkilder, og er ikke mulig å planlegge i motsetning til vannkraftanlegg og kraft produsert ved å brenne fossilt brensel. For å nøyaktig vurdere bidraget intermitterende fornybare energikilder har på et kraftsystem trengs en metode for å kvantifisere integrasjonen i et eksisterende kraftsystem.

Denne avhandlingen presenterer og forklarer en metode som kvantifiserer Capacity Value (CV) av vindkraftanlegg som integreres i eksisterende sammensatte kraftsystem. Avhandlingen er ment som et bidrag til det pågående Power System Reliability-prosjektet ved Instituttet for Elkraftteknikk ved NTNU. Kraftsystemets probabilistiske natur simuleres ved hjelp av State Sampling-metoden, som er en Monte Carlo Simululerings-metode (MCS), og Capacity Value-markøren Effective Load Carrying Capability (ELCC) er bestemt ved å bruke halvdelingsmetoden (bisection method).

Et internt dataprogram som er i stand til å kvantifisere verdien av ELCC for vindkraftanlegg som integreres i sammensatte kraftsystemer er utviklet som en del av denne avhandlingen. Programmet kan basere ELCC kalkuleringene på to forskjellige pålitelighetsmarkører, LOLE og EENS. Ved å bruke to forskjellige markører for å bestemme ELCC av tillagt kraftproduksjon i sammensatte kraftsystemer er det vist at det produseres forskjellige perspektiver av mulige kraftsystemekspansjoner.

Gjennom et litteraturstudie presenterer avhandlingen en dyptgående forklaring av pålitelighetsstudier av kraftsystemer. Både sekvensielle og ikke-sekvensielle MCS metoder er forklart i detalj. MCS metoden State Sampling er brukt i dataprogrammet utviklet igjennom denne avhandlingen, da denne metoden viste seg å trenge færre simuleringsår for å konvergere mot et resultat enn State Duration- og State Transition-metodene.

Acknowledgement

I want to express my thanks to my supervisor, Associate Professor Vijay Venu Vadlamudi, Department of Electric Power Engineering, NTNU. His help, guidance and understanding this last year has been invaluable, as this period has been a challenging part of my life. I would also like to thank Kristoffer Halseth for his guidance and NTNU for their flexibility and understanding.

Trondheim, 01.08.2022

Martin Widding

Table of Contents	Page
Abstract	i
Sammendrag	ii
Acknowledgement	iii
Table of Contents	vii
Abbreviations	ix
List of Figures	x
List of Tables	xiii
1 Introduction	1
1.1 Background	1
1.2 Scope	1
1.3 Project contributions	2
1.4 Project structure	2
2 The Fundamentals of Power System Reliability	4
2.1 General Elements of PSR	4
2.1.1 Power System Reliability Studies	4
2.1.2 Hierarchical Level	5
2.1.3 Generation Adequacy Assessment	7
2.1.4 Component Unavailability	7
2.1.5 Load Model	8
2.1.6 COPT	10
2.2 Reliability Indices	13
2.2.1 Loss of Load Probability	14
2.2.2 Loss of Load Expectation	15
2.2.3 Loss of Load Frequency	16
2.2.4 Expected Energy Not Served	17
2.3 Monte Carlo Simulation	20
2.3.1 MCS Basics	20
2.3.2 State Sampling Method	21
2.3.3 State Duration Method	21
2.3.4 State Transition Method	24
2.4 Capacity Value and Wind Power integration	28
2.4.1 Capacity Value	28
2.4.1.1 Effective Load Carrying Capability	29
2.4.2 Equivalent Firm Capacity and Equivalent Conventional Capacity	31

2.4.3	Wind Generation Modelling	32
2.4.3.1	Wind Speed Modelling	32
2.4.3.2	Wind Turbine Generator Modelling	34
2.4.3.3	Wind Farm Modelling	35
2.5	Composite systems	37
2.5.1	Introduction	37
2.5.2	General Elements	38
2.5.2.1	Input Data	38
2.5.2.2	System State	39
2.5.3	Isolated buses and contingency solvers	39
3	Methodological Approach	41
3.1	Load Model	42
3.1.1	Standard Load Model	42
3.1.2	Increasing the load by ΔL	45
3.2	State Sampling	47
3.3	Wind Power Integration	50
3.4	Bisection Method	51
3.5	ELCC based on LOLE	54
3.6	ELCC based of EENS	54
4	Case Studies and Results	55
4.1	MRBTS	56
4.2	Obtaining the CV of test systems using LOLE as basis for ELCC calculations	57
4.2.1	RBTS	57
4.2.2	MRBTS	58
4.2.3	RTS	59
4.2.4	Summation and discussion of results where LOLE is used as basis for ELCC calculations	60
4.3	Obtaining the CV of test systems using EENS as basis for ELCC calculations	62
4.3.1	RBTS	62
4.3.2	MRBTS	63
4.3.3	RTS	64
4.3.4	Summation and discussion of results where EENS is used as basis for ELCC calculations	65
4.4	Comparison of LOLE and EENS used as a basis for ELCC	66
5	Conclusions and Future Work	67
5.1	Conclusions	67
5.2	Future Work	68
	References	73

Appendices	74
A COPT Example Code	74
B MCS Example codes	76
B.1 Example State Duration	76
B.2 Example State Transition	78
C RBTS	80
C.1 RBTS Topology, single line diagram	80
C.2 RBTS Generator data	81
C.3 RBTS Network data	81
C.4 RBTS Bus data	82
D IEEE-RTS	83
D.1 RTS Topology, single line diagram	83
D.2 RTS Generator data	84
D.3 RTS Network data	85
D.4 RTS Bus data	87
E Individual bus reliability indices and standard deviation when ELCC is based on LOLE	88
E.1 RBTS	88
E.2 MRBTS	88
E.3 RTS	89
F Individual bus reliability indices and standard deviation when ELCC is based on EENS	90
F.1 RBTS	90
F.2 MRBTS	90
F.3 RTS	91
G Coefficients of variation for individual buses when ELCC is based on LOLE	92
G.1 RBTS	92
G.2 MRBTS	92
G.3 RTS	93
H Coefficients of variation for individual buses when ELCC is based on EENS	94
H.1 RBTS	94
H.2 MRBTS	94
H.3 RTS	95

Abbreviations

BESS Battery Energy Storage System.

COPT Capacity Outage Probability Table.

CV Capacity Value.

CYPL Constant Yearly Peak Load.

DPL Daily Peak Load.

ECC Equivalent Conventional Capacity.

EENS Expected Energy Not Served.

EES Electric Energy Source.

EFC Equivalent Firm Capacity.

ELCC Effective Load Carrying Capability.

FOR Forced Outage Rate.

HL Hierarchical level.

IEEE-RTS Institute of Electrical and Electronics Engineers - Reliability Test System.

LOL Loss of Load.

LOLE Loss of Load Expectation.

LOLF Loss of Load Frequency.

LOLP Loss of Load Probability.

MCS Monte Carlo Simulation.

MRBTS Modified Roy Billinton Test System.

MTTF Mean Time to Failure.

MTTR Mean Time to Repair.

OPF Optimal Power Flow.

PSR Power System Reliability.

RBTS Roy Billinton Test System.

RES Renewable Energy Sources.

TTF Time to Failure.

TTR Time to Repair.

WECS Wind Energy Conversion System.

WPL Weekly Peak Load.

WTG Wind Turbine Generator.

YPL Yearly Peak Load.

List of Figures

2.1.1 Hierarchical levels of the power system. [6]	5
2.1.2 Examples of load duration curves for an overall year with different load increments.[15, 18]	9
2.1.3 Examples of chronological peak load curves for an overall period of one year with different load increment.[15, 18]	10
2.2.1 Illustration of the HL-II risk model [6]	13
2.3.1 Total generation capacity during the steps of the state duration method example	23
2.3.2 Example of state duration method, state of the components	24
2.3.3 Visualization of state transition method	25
2.3.4 Total generation capacity during the state duration example	27
2.3.5 Example of state transition method, state of the components	27
2.4.1 Power Curve of wind turbine [7]	34
3.2.1 A flowchart showing how the State Sampling method is used. [7]	49
3.4.1 Illustration of the bisection method [34]	51
3.4.2 Example showing the bisection interval of a illustrative system	54
4.1.1 Single line diagram of the MRBTS [7]	56
4.2.1 Bar chart comparing the $ELCC_{LOLE}$ [%] of the test systems.	60
4.3.1 Bar chart comparing the $ELCC_{EENS}$ [%] of the test systems.	65

List of Tables

2.1.1 Example of a COPT	11
2.3.1 Data used in state duration example	22
2.3.2 Results of state duration method example	23
2.3.3 Results of state transition method example	26
2.5.1 Line input data, State Sampling AC-solver. [6]	38
2.5.2 Generator input data, State Sampling AC-solver. [6]	38
2.5.3 Bus specification, AC-solver. [6]	39
3.1.1 The weekly peak load, used to obtain the load model of the system	43
3.1.2 The daily peak load, used to obtain the load model of the system	43
3.1.3 The hourly peak load, used to obtain the load model of the system	44
3.3.1 WECS transmission line data [7]	50
3.3.2 Wind speed data for Ørland [7]	50
3.3.3 Estimated Weibull parameters for the Ørland wind regime [7]	50
4.2.1 Comparison of LOLE and EENS between the RBTS and the RBTS-WL when ELCC is based on LOLE	57
4.2.2 The $ELCC_{LOLE}$ of added wind power generation integrated in the RBTS-WL	57
4.2.3 Comparison of LOLE and EENS between the MRBTS and the MRBTS-WL when ELCC is based on LOLE	58
4.2.4 The $ELCC_{LOLE}$ of added wind power generation integrated in the MRBTS-WL	58
4.2.5 Comparison of LOLE and EENS between the RTS and the RTS-WL when ELCC is based on LOLE	59
4.2.6 The $ELCC_{LOLE}$ of added wind power generation integrated in the RTS-WL	59
4.2.7 Summation of $ELCC_{LOLE}$ calculations applied to the different test systems	60
4.3.1 Comparison of LOLE and EENS between the RBTS and the RBTS-WL when ELCC is based on EENS	62
4.3.2 The $ELCC_{EENS}$ of added wind power generation integrated in the RBTS-WL	62
4.3.3 Comparison of LOLE and EENS between the MRBTS and the MRBTS-WL when ELCC is based on EENS	63
4.3.4 The $ELCC_{EENS}$ of added wind power generation integrated in the MRBTS-WL	63
4.3.5 Comparison of LOLE and EENS between the RTS and the RTS-WL when ELCC is based on EENS	64
4.3.6 The $ELCC_{EENS}$ of added wind power generation integrated in the RTS-19	64
4.3.7 Summation of $ELCC_{EENS}$ calculations applied to the different test systems	65
C.2.1RBTS generator data	81
C.3.1RBTS network parameters	81
C.3.2RBTS outage data	82
C.4.1RBTS Bus data	82
D.2.1RTS generator data	84
D.3.1RTS network parameters	85

D.3.2	RTS outage data	86
D.4.1	RTS Bus data	87
E.1.1	The individual bus indices for the RBTS, when ELCC is produced with LOLE as the basis. These results are a product of the RBTS analysis preformed in Chapter 4.2.1. These are the indices of the new system, not including the benchmark system. "std" refers to the standard deviation. . .	88
E.2.1	The individual bus indices for the MRBTS, when ELCC is produced with LOLE as the basis. These results are a product of the MRBTS analysis preformed in Chapter 4.2.2. These are the indices of the new system, not including the benchmark system. "std" refers to the standard deviation. . .	88
E.3.1	The individual bus indices for the RTS, when ELCC is produced with LOLE as the basis. These results are a product of the RTS analysis preformed in Chapter 4.2.3. These are the indices of the new system, not including the benchmark system. "std" refers to the standard deviation.	89
F.1.1	The individual bus indices for the RBTS, when ELCC is produced with EENS as the basis. These results are a product of the RBTS analysis preformed in Chapter 4.3.1. These are the indices of the new system, not including the benchmark system. "std" refers to the standard deviation. . .	90
F.2.1	The individual bus indices for the MRBTS, when ELCC is produced with EENS as the basis. These results are a product of the MRBTS analysis preformed in Chapter 4.3.2. These are the indices of the new system, not including the benchmark system. "std" refers to the standard deviation. . .	90
F.3.1	The individual bus indices for the RTS, when ELCC is produced with EENS as the basis. These results are a product of the RTS analysis preformed in Chapter 4.3.3. These are the indices of the new system, not including the benchmark system. "std" refers to the standard deviation.	91
G.1.1	The coefficient of variation for the different buses when ELCC is produced with LOLE as the basis. Resulting from the RBTS analysis preformed in Chapter 4.2.1. BM refers to the benchmark system, NS refers to the new system where wind power generation is integrated and the load is increased.	92
G.2.1	The coefficient of variation for the different buses when ELCC is produced with LOLE as the basis. Resulting from the MRBTS analysis preformed in Chapter 4.2.2. BM refers to the benchmark system, NS refers to the new system where wind power generation is integrated and the load is increased.	92
G.3.1	The coefficient of variation for the different buses when ELCC is produced with LOLE as the basis. Resulting from the RTS analysis preformed in Chapter 4.2.3. BM refers to the benchmark system, NS refers to the new system where wind power generation is integrated and the load is increased.	93

- H.1.1 The coefficient of variation for the different buses when ELCC is produced with EENS as the basis. Resulting from the RBTS analysis preformed in Chapter 4.3.1. BM refers to the benchmark system, NS refers to the new system where wind power generation is integrated and the load is increased. 94
- H.2.1 The coefficient of variation for the different buses when ELCC is produced with EENS as the basis. Resulting from the MRBTS analysis preformed in Chapter 4.3.2. BM refers to the benchmark system, NS refers to the new system where wind power generation is integrated and the load is increased. 94
- H.3.1 The coefficient of variation for the different buses when ELCC is produced with EENS as the basis. Resulting from the RTS analysis preformed in Chapter 4.3.3. BM refers to the benchmark system, NS refers to the new system where wind power generation is integrated and the load is increased. 95

1 Introduction

1.1 Background

Worldwide, electric power systems are developing and evolving to meet the needs of a growing population with an increasing dependency on electricity. The emergence of personal computers, cell phones, and more lately the embrace of electric cars has put pressure on the existing power supply and infrastructure, as new developments increase and change the demand for power. To accommodate this demand, in addition to the well documented global environmental issues, the search for cost effective Renewable Energy Sources (RES) has been intensified. In the last decade, wind and solar photovoltaic power (PV) has been the largest growing RES on the market [1, 2]. However, using these sources to generate power is different from burning fossil fuels, nuclear fission and operation of large dams. Solar power is only available at daytime, and wind power fluctuates both from hour to hour as well as season to season. The need for robust power systems to ensure secure supply of power as well as power system flexibility is therefore more important than ever [3]. The reliability of the energy system needs to be weighted against economic criteria. This creates a demand for dependable and objective tools to assess the adequacy of energy systems where these intermittent energy sources are implemented.

Reliability assessments of energy systems is a developed field, which there exist a great amount of research on. Historically, these studies have applied analytical methods, such as the state space method and minimal cut set method. The disadvantage of analytical methods is both their need to simplify large systems, and their deterministic approach [4]. To capture the random nature of a power system, the standard approach has been to apply a stochastic method named Monte Carlo Simulation (MCS) [5].

When integrating a intermittent power source into an existing power system, it is important to quantify the impact of the added generation. The Capacity Value (CV) of the added generation has become relevant information when comparing different expansions of the power system.

1.2 Scope

This thesis is based on the work done in a specialization project Autumn 2020. The focus of this project was to develop an understanding of the fundamentals of power system reliability studies, Capacity Value and wind power integration in HL-I and HL-II. With the specialization project as a basis, the thesis work conducted in Spring 2022 is stated in the follow problem statement:

- To create a framework for assessing the Capacity Value of added wind power generation to an existing power system. To identify/select/create suitable methodology for the PSR assessment in HL-II. Further develop the in-house software for obtaining the Capacity Value of wind power generation added to a system.

The thesis aims to develop methods of obtaining CV. MCS optimization such as variance reduction and computational efficiency has not been included.

1.3 Project contributions

- The work done through this thesis is an addition to the software developed at the Department of Electrical Power Engineering at NTNU. This software is an ongoing project focused at developing a comprehensive framework for performing PSR assessments on power systems. The goal of this extension of the pre-existing software is to evaluate the Capacity Value of wind power added to an existing composite system. Both Loss of Load Expectation (LOLE) and Expected Energy Not Served (EENS) are selected as basis for the Capacity Value evaluation and Effective Load Carrying Capability (ELCC) is selected as the CV metric used in this thesis. The reliability indices of the power system will be evaluated through preexisting software presented in the Master's theses [6] and [7] from the Department of Electric Power Engineering at NTNU. The CV of the system will be obtained through MATLAB software developed as part of this thesis work.
- The methodology presented and applied in this thesis is a combination of different methods found in literature regarding power system reliability studies, capacity value and wind modelling to reach the objective stated. The theories behind these concepts are explored through the thesis work to clarify the choices made throughout the development of the software presented.
- The thesis work presented is written with the goal of presenting information on PSR in a clear and concise manner. In doing so it is intended to be a viable tool used for further development of the ongoing PSR project at the Department of Electrical Power Engineering at NTNU.

1.4 Project structure

Chapter 1 - *Introduction* - includes the projects background, scope, contribution and its structure.

For establishing narrative clarity and with an aim to make this thesis a complete and independent unit in and of itself, much of the content from chapter 2 and some of the content of chapter 1 is a replication of the specialisation project work, with suitable extensions where deemed necessary.

Chapter 2 - *Fundamental of PSR studies* - includes the fundamentals for understanding power system reliability studies in HL-I and HL-II. It introduces the reliability indices, Monte Carlo Simulation, Capacity Value, and the fundamentals of wind generation modelling.

Chapter 3 - *Methodological Approach* - presents explanations on the method utilized to compute the CV of an HL-II system. This part highlights the unique contributions made in the thesis work, mainly the method used to increase the load and the bisection method, and states which parts are replications of pre-existing work.

Chapter 4 - *Case Studies and Results* - utilizes the software developed in the thesis work to calculate the ELCC of different test systems based on both LOLE and EENS. This chapter presents the results and discusses the differences between the two indices used as basis for ELCC.

Chapter 5 - *Conclusion and future work* - includes a summary of the work of the thesis and proposes future work.

2 The Fundamentals of Power System Reliability

This thesis work aims to develop software capable of obtaining the CV of added wind power generation to an existing power system in HL-II. To present a clear and cohesive narrative, a comprehensive literature study on power system reliability has been done, and is presented in this chapter.

2.1 General Elements of PSR

This chapter presents the fundamentals of PSR adequacy studies. It addresses the reliability definition, the definition of generation adequacy, as well as the probabilistic and deterministic methods. The definition of component unavailability, the load model and the Capacity Outage Probability Table (COPT) are introduced. These concepts and definitions are important to address, as they are essential to understand and define the PSR study completed in this thesis.

2.1.1 Power System Reliability Studies

The objective of an electric power system is to provide the consumer with adequate and continuous power. This translates to a continuous reception of expected energy over an extended time period to the customer. The delivered energy should fulfill the requirements and standards of its operating region. The power system's reliability is measured based on the frequency, duration, and magnitude of the disruptive events on the power supplied to the end consumer [8, 9].

There are two main facets of power system reliability; system security and system adequacy. Security is defined as the power system's ability to withstand the risk of short term contingencies, while adequacy is defined as the system's ability to meet the long term demands [10]. The two terms are specified in several documents from International Council on Large Electric Systems (CIGRE) [9].

1. *"Adequacy – The ability of the power system to supply the aggregate electric power and energy requirements of the customer at all times, taking into account scheduled and unscheduled outages of system components."*
2. *"Security – The ability of the power system to withstand sudden disturbances such as electric short circuits or non-anticipated loss of system components."*

Security relates to the dynamic conditions of the power system, referring to the operation of the system. Adequacy relates to the the static conditions of the power system, referring to the planning process of the system [10]. The term *reliability* is often used to explain *adequacy*. This distinguishes reliability from security, as the definition of adequacy does not cover the entire operation of ensuring reliability of an electric power system, as defined in International Electrotechnical Commission [11]. ” *The reliability of an electric power system is defined as the probability that an electric power system can perform a required function under given conditions for a given time interval*”. Although the perception of equating reliability with adequacy is theoretically incorrect, the evaluation of power system reliability in this thesis will be based on the system’s adequacy [12].

2.1.2 Hierarchical Level

Power system reliability studies can be categorized into different hierarchical levels, which are defined by the functional zone related to the segments of the power system. Figure 2.1.1 shows the functional zones, which are the boundaries of the reliability assessment. By utilizing these functional zones, one can distinctly limit the scope of a study to include parts of the power system. A completely realistic representation of the system would result in a complex model which would be challenging to calculate. This is why most analytical methods simplify the system. When preforming a HL-III study the distribution subsystem is usually evaluated separately from the transmission and generation subsystems [12].

This thesis will address the HL-II representation of the power system.

The illustration presented in Figure 2.1.1 visually illustrates the hierarchical levels. The functional zones are Generation, Transmission, and Distribution facilities.

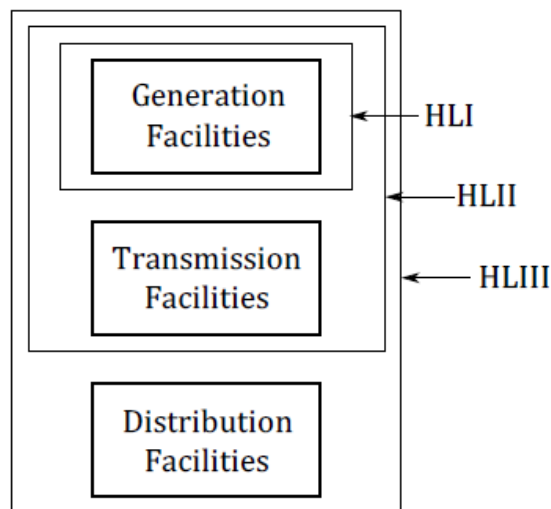


Figure 2.1.1: Hierarchical levels of the power system. [6]

HL-I includes the generation and load of the system. Conducting a reliability study of level I, includes the generation capacity of the total system, in order to satisfy the load demanded of the power system [6, 12].

HL-II includes the load, generation and transmission facilities, and refers to the "bulk power system" and its ability to sufficiently supply the system load [6, 12].

HL-III includes the entire system, adding the distribution facilities to HL-II. This includes the ability to generate and transfer energy to the end-consumer. Conducting a reliability study of HL-III is difficult due to the complexity and size of power systems. A reliability study of HL-III is only practical for small systems or by isolating the distribution facilities and disregarding generation and transmission [6, 12].

2.1.3 Generation Adequacy Assessment

As established in 2.1.1, reliability assessment can be divided into security assessment and adequacy assessment. This thesis evaluates the PSR based on the system's adequacy assessment. The system's adequacy can further be evaluated using two different approaches; the deterministic approach and the probabilistic approach [13].

The deterministic and probabilistic approaches can be differentiated by the probabilistic method's use of randomness to simulated a systems behaviour. Using an initial set of conditions for a probabilistic model will give different results every time the model is computed, as it relies on random number generation. Utilising the same input for a deterministic model would result in an output that remains unchanged through multiple computations.

The deterministic approach in PSR studies estimates the available generation and capacity of the network. This approach does not assume any uncertainty or variability in the system, which can be inaccurate as a real power system is stochastic in nature [13].

The probabilistic approach in PSR studies estimates the probability of the system's incapability to supply the demand [14]. The probabilistic approach can further be divided into simulation methods and analytical methods.

The analytical approach uses mathematical techniques to directly solve the numerical solution resulting in the reliability indices of a system. The simulation approach is used when the analytical formulation cannot be derived, or the formulation demands too many simplifications, resulting in an inaccurate model. Monte Carlo Simulation is a simulation method often used in PSR [6]. It is based on random number generation, and is the method utilised in this thesis to estimate the reliability indices of a given system. This is performed by simulating the random behaviour of the system [15], and is further elaborated in Chapter 2.3. The reliability indices of the probabilistic approach will be further elaborated in Chapter 2.2.

2.1.4 Component Unavailability

In the occurrence of an outage of a generating unit, the unit must be removed from service to be either replaced or repaired. These outages can be harmful, since they affect the system's ability to supply load, which subsequently diminishes the system's reliability. An outage can be separated into two categories; forced outage and planned outage. A case defined as forced outage is the result of sudden conditions where a unit is forced to be removed to secure operation of the remaining system. A planned outage is mainly when units are removed due to maintenance and is not included in the scope of this thesis [16].

The probability of finding a unit on forced outage is defined as the unit unavailability and is represented as the Forced Outage Rate (FOR) in power system reliability studies. FOR is expressed by Equation 2.1 and the Availability is expressed by Equation 2.2 [17].

$$\begin{aligned} \text{Unavailability}(FOR) = U &= \frac{\lambda}{\lambda + \mu} = \frac{r}{m + r} = \frac{r}{T} \\ &= \frac{f}{\mu} = \frac{\Sigma[\text{Down Time}]}{\Sigma[\text{Down Time}] + \Sigma[\text{Up Time}]} \end{aligned} \quad (2.1)$$

$$\begin{aligned} \text{Availability} &= \frac{\mu}{\lambda + \mu} = \frac{m}{m + r} = \frac{m}{T} \\ &= \frac{f}{\lambda} = \frac{\Sigma[\text{Up Time}]}{\Sigma[\text{Down Time}] + \Sigma[\text{Up Time}]} \end{aligned} \quad (2.2)$$

where

- λ = expected failure rate
- μ = expected repair rate
- m = mean time to failure (MTTF) = $1/\lambda$
- r = mean time to repair (MTTR) = $1/\mu$
- $m + r$ = mean time between failures (MTBF) = $1/(\lambda + \mu)$
- f = cycle frequency
- T = cycle time

The *Up Time* and *Down Time* refers to the state of a unit in a two-state model assumed for this operation, applicable to a base load generating unit. This can be translated to the unit being in service during *Up Time* and on forced outage during *Down Time*. A multi-state model allows the representation of partial states of unavailability. Various states of such a model are referred to as derated states. States such as "reserve shutdown" and "forced out but not needed" are possible in a multi-state model, and described further in [17]. This thesis will evaluate the components of the power system using the two-state model.

2.1.5 Load Model

A system's load over a specific period of time can be represented by a load model. This model describes the load variations over a given time period, e.g. one day, one year, or several years, and is based on historical data. The time period can be divided into increments of equal duration. Each increment consist of a singular load value, and the duration of each time increment directly determines the load model's accuracy. The Constant Yearly

Peak Load (CYPL) (or often simply referred to as the Yearly Peak Load (YPL)) is a load model where the load is represented as the peak annual load of the system. This load model will produce a single load value, with the duration of a year. This will lead to a pessimistic result, but will also result in a reduced time to compute or calculate. A more accurate approximation is the Weekly Peak Load (WPL) that includes 52 time increments where each increment can have different load levels. More accurate load models than WPL are e.g. Daily Peak Load (DPL), where the time period is divided into individual days, and Hourly Peak Load (HPL) where the time period is divided into individual hours [18]. The HPL method will be used in the software developed in this thesis. How it is used is further explained in 3.1.

Figure 2.1.2 illustrates how the load models becomes more accurate and descriptive of the actual load of a system when the number of time increments is increased. In this figure each load level is represented according to size. Each of these curves are known as a peak load duration curve [17, 18] of a given system. The peak loads can also be stated in a chronological representation, where a specified time interval is represented by a specific load level. This is illustrated in Figure 2.1.3. The load forecast uncertainty is not considered in this thesis, and the load model used are only predictions of future loads based on historical data [15, 18]. The curves in Figure 2.1.2 and 2.1.3 are meant to illustrate the possible load models, thus not representing any specific data or system.

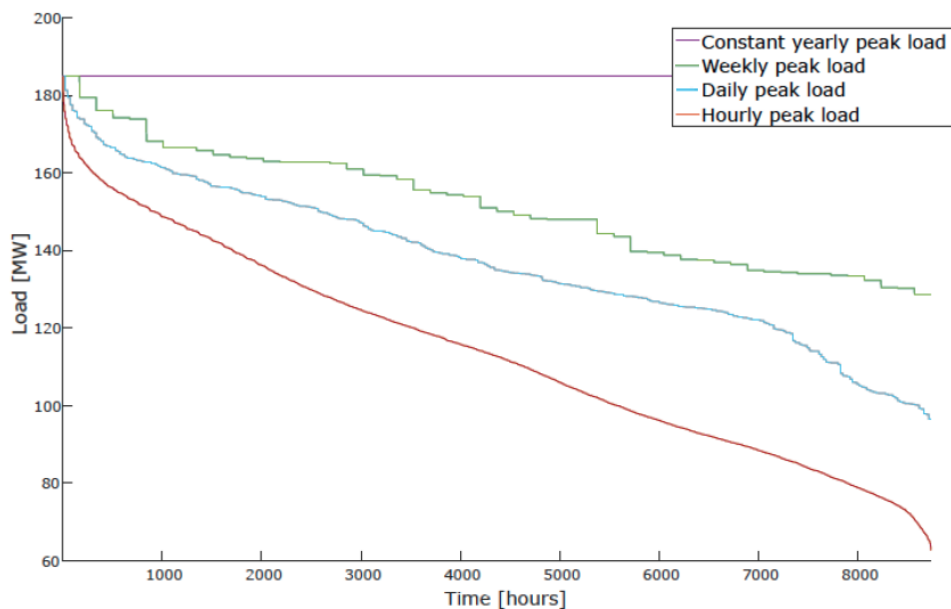


Figure 2.1.2: Examples of load duration curves for an overall year with different load increments.[15, 18]

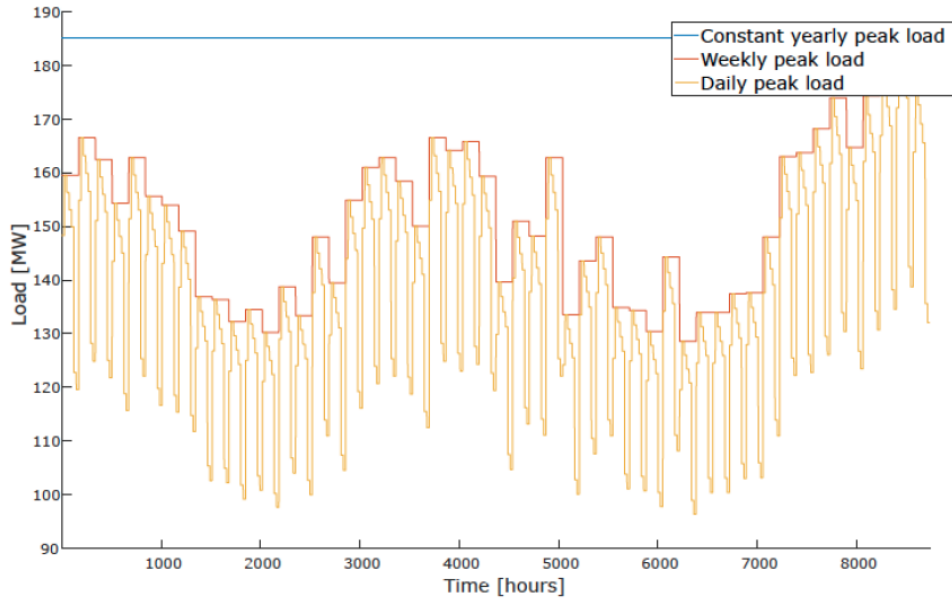


Figure 2.1.3: Examples of chronological peak load curves for an overall period of one year with different load increment.[15, 18]

2.1.6 COPT

A generation model commonly used in PSR studies is the Capacity Outage Probability Table (COPT). The COPT is a table containing the possible outage states of a generation system in ascending order. The table consists of the capacity outage levels x_j , given in power quantity, their corresponding cumulative probability $P(X \geq x_j)$ and individual probability $p(X = x_j)$ of being on outage. The individual probability shows the probability that the specific state x_j is on outage, while the cumulative probability shows the probability that an amount greater or equal to the x_j capacity is on outage. The cumulative probability can be expressed by Equation 2.3. The equation shows that the cumulative probability is given by the sum of the individual probabilities of all states where the outage of power is X or larger. C is denoted as the total installed capacity in the system [19, 15, 18].

$$P(X \geq x_j) = \sum_{X=x_j}^C p(X) \quad (2.3)$$

Equation 2.3 can be utilized if the individual probability of each state is given, whereas using a recursive algorithm can calculate the cumulative probability directly. The algorithm is expressed in Equation 2.4; calculating the cumulative probability of a capacity outage when a capacity unit has been added [15, 18].

$$P(X \geq x_j) = (1 - FOR) \cdot P'(X \geq x_j) + FOR \cdot P'(X \geq x_j - g) \quad (2.4)$$

$P'(x)$ is the cumulative probability of the old COPT and g is the newly added capacity unit. Equation 2.5 solves the cases when the cumulative probability function can become zero or negative [15, 18].

$$P'(X \geq x_j) = 1 \text{ for } \begin{cases} x_j \leq 0 \\ x_j - g \leq 0 \end{cases} \quad (2.5)$$

The recursive algorithm in Equation 2.4 can be modified to represent the derated system. In Equation 2.6, a new unit with i states has been added. Every time a new unit is added to the probability distribution, a new COPT is created. This means that all previous outage states are updated and the new outages are added. In the equation, n is denoted as the number of unit states, implying that if $n = 2$, Equation 2.6 would be reduced to Equation 2.4 [15, 17].

The multi-state representation for generation units is expressed by Equation 2.6 [15, 18].

$$P(X \geq x_j) = \sum_{i=1}^n p_i \cdot P'(X \geq x_j - g_i) \quad (2.6)$$

p_i is the probability of the new unit being in state i , while g_i is the capacity of the new unit being in state i .

Table 2.1.1: Example of a COPT

State j	Capacity outage x_j [MW]	Individual prob. $p(X = x_j)$	Cumulative prob. $P(X \geq x_j)$
0	0	0.941192	1.000000
1	5	0.038416	0.058808
2	10	0.019600	0.020392
3	15	0.000784	0.000792
4	20	0.000008	0.000008

An example of a COPT is shown in Table 2.1.1, inspired by Billinton [17], but modified with new values. The calculation follows the expression given in Equation 2.4.

The system considered in this example includes three generation units of 5 MW, 5 MW, and 10 MW generation capacity with an identical FOR of 0.02 for all three units. The following steps are similar to the approach in [17]. These are included to illustrate the procedure used in the MATLAB script that is attached to Appendix A. The COPT in Table 2.1.1 was created sequentially as follows:

1. Adding the first unit of 5 MW

$P(0) = (1-0.02)(1)$	$+(0.02)(1.0)$	$= 1$
$P(5) = (1-0.02)(0)$	$+(0.02)(1.0)$	$= 0.2$

2. Adding the second unit of 5 MW

$P(0) = (1-0.02)(1)$	$+(0.02)(1.0)$	$= 1$
$P(5) = (1-0.02)(0.02)$	$+(0.02)(1.0)$	$= 0.0396$
$P(10) = (1-0.02)(0)$	$+(0.02)(0.02)$	$= 0.0004$

3. Adding the third unit of 10 MW

$P(0) = (1-0.02)(1)$	$+(0.02)(1.0)$	$= 1$
$P(5) = (1-0.02)(0.0396)$	$+(0.02)(1.0)$	$= 0.058808$
$P(10) = (1-0.02)(0.004)$	$+(0.02)(1.0)$	$= 0.020392$
$P(15) = (1-0.02)(0)$	$+(0.02)(0.0396)$	$= 0.000792$
$P(20) = (1-0.02)(0)$	$+(0.02)(0.004)$	$= 0.000008$

The calculation for each step follows the method expressed in Equation 2.4, and shows the cumulative probability of a specific outage state after an unit of capacity and its FOR is added to the system. Step 3 shows the cumulative values given in the COPT shown in Table 2.1.1. A state's individual probability of being on outage is the sum of its corresponding cumulative probability subtracted with the succeeding cumulative probability of the next state.

2.2 Reliability Indices

The most common probabilistic indices of PSR applicable for HL-I and HL-II assessment are based on Loss of Load (LOL) events in the system. The LOL indices introduced are essential for evaluating generation adequacy. LOL is associated with insufficient generation in HL-I studies, meaning that the generation units are unable to supply the load demanded at a given time [6, 13]. In HL-II studies, LOL is associated with the inability to supply the load demanded at a given time, due to restrictions in generation and/or transmission capacity. *Loss of Load* and *Capacity Outage* is commonly mentioned when discussing reliability indices, but it should be noted that these terms does not describe the same event. *Loss of Load* will occur when the system load level exceeds the capability of the generating capacity still in service. *Capacity Outage* would indicate a loss of generation, but this does not necessarily mean that it results in a loss of load as it is dependant on the generating capacity reserve and the system load level [17].

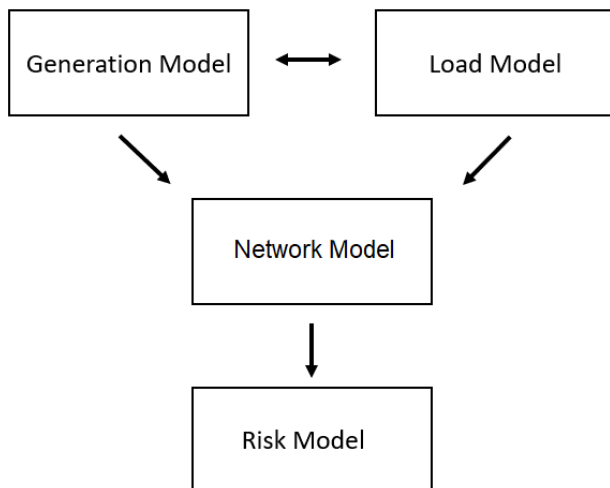


Figure 2.2.1: Illustration of the HL-II risk model [6]

The development of the risk model consists of three parts as shown in Figure 2.2.1. The illustration [6] shows the main elements of the development of the risk model for HL-II studies. For HL-I studies, the figure would be similar, except that the network model would not be included. The risk model is used to calculate the system adequacy indices, where the most commonly utilised indices are Loss of Load Probability (LOLP) and Loss of Load Expectation (LOLE). The names used for reliability indices are many, and are sometimes referred to as *risk* indices. Risk takes into account the severity and probability of a hazardous event. This is why reliability indices are used in probabilistic approaches as the deterministic approach can only consider the severity of a hazardous event, not the likelihood of its occurrence [17].

Risk models can have different fields of usage because the load model chosen (e.g. HPL, CYPL) will determine the unit for the loss of load index. This means that the load model based on the daily peak load determines the unit for loss of load index as days/year, whereas a load model based on hourly peak load determines a loss of load index in hours/year [13, 18].

This thesis introduces adequacy indices connected to loss of load events. These are Loss of Load Probability (LOLP), Loss of Load Expectation (LOLE) and Loss of Load Frequency (LOLF). It also introduces a reliability index which is based on the severity of loss of load events. This index is known as Expected Energy Not Served (EENS) [14]. The software developed in this thesis will be focused on obtaining and utilizing LOLE and EENS.

For the following calculations in this chapter, the mathematical expressions presented for the indices includes a format for both the analytical calculation method and for the simulation method.

2.2.1 Loss of Load Probability

The loss of Load Probability (LOLP) is the probability that a loss of load event occurs for a given period of time. For HL-I studies, the reason for the LOL event is that the load is exceeding the available generation in the system, which would be a consequence of either unit outage or unexpected increase in demand. For HL-II studies, the reason is that the system is unable to supply the load at a location, due to either inadequate generation or inability to transfer power to the location in question. As previously mentioned, the LOLP index is the calculation of COPT and load model convolved [15].

When regarding HL-I studies Equation 2.7 can be used. In a situation where loss of load occurs, the systems load and the total capacity outage would exceed the installed capacity. The LOLP value of the analytical method is represented in Equation 2.7 [15].

$$LOLP_t = (X > C - L_t) \quad (2.7)$$

The chosen time increment is represented as t , X is the outage capacity, C is the installed capacity of the system, and L_t is the load at given time increment.

LOLP can also be represented by summing all probabilities of system states with loss of load expressed mathematically in Equation 2.8 [14].

$$LOLP = \sum_{i \in S} p_i \quad (2.8)$$

S represents the set of system states with loss of load while p_i is the probability of occurrence of the state.

A “re-engineered” version of Equation 2.8 for MCS can be obtained when the load requirement is constant through the period studied, and is expressed below in Equation 2.9. It is similar to Equation 2.8 but is applied in a different format to adjust for the simulation method. When applying MCS, the system states are sampled in the simulation, where a state is obtained for each time increment of a simulation year. A simulation will normally include multiple years simulated. Reliability indices are calculated for each simulation year resulting in these indices becoming averages of the yearly indices. Dividing the sum of these yearly indices by the number of simulation years N multiplied by the number of time increments M gives the expression of LOLP for MCS given below in Equation 2.9. Δt is the duration of the time increment and x_j is the outcome of each time increment (0 or 1). 1 equals LOL while 0 equals adequate state [14, 6].

$$LOLP_{MCS} = \frac{\sum_{i=1}^N (\sum_{j=1}^M x_j \cdot \Delta t)}{N \cdot M} \quad (2.9)$$

2.2.2 Loss of Load Expectation

The Loss of Load Expectation (LOLE) index gives the expected number of time units where loss of load events will occur for a specific time period. The LOLE risk index is the most commonly used probabilistic method in power generation evaluation because it is well adapted to consider system expansions and interconnections [16]. The unit of the index LOLE depends on the study period as it is common to calculate the index in terms of *days/year* or *hours/year*. As mentioned previously, the unit must equate the load model utilized. Equation 2.10 and Equation 2.11 express the definition of LOLE for the analytical method. These equations can also be further derived as a rewritten equation with the inclusion of LOLP as expressed in Equation 2.7 at a given time increment. These rewritten equations are expressed in Equation 2.12 and Equation 2.13 [15, 18].

$$LOLE = \sum_{t=1}^{365} P(X > C - L_t) \cdot \Delta t \left[\frac{\text{days}}{\text{year}} \right] \quad (2.10)$$

$$LOLE = \sum_{t=1}^{8760} P(X > C - L_t) \cdot \Delta t \left[\frac{\text{hours}}{\text{year}} \right] \quad (2.11)$$

$$LOLE = \sum_{t=1}^{365} LOLP_t \cdot \Delta t \left[\frac{\text{days}}{\text{year}} \right] \quad (2.12)$$

$$LOLE = \sum_{t=1}^{8760} LOLP_t \cdot \Delta t \left[\frac{\text{hours}}{\text{year}} \right] \quad (2.13)$$

The duration of the time increment ΔT is dependant on the load model used e.g 1 day for Daily Peak Load (DPL) and 1 hour for Hourly Peak Load (HPL)[15].

In Equation 2.8, LOLE can similar to LOLP be represented by summing for all probabilities of system states with loss of load. This time it is multiplied with the evaluation time period T . The expression is presented mathematically in Equation 2.14 [14].

$$LOLP = \sum_{i \in S} p_i \cdot T \quad (2.14)$$

Similar to Chapter 2.2.1 when applying MCS, the "re-engineered" version of Equation 2.14 is presented below in Equation 2.15. The MCS adjusted expression for LOLE divides the sum of yearly indices by the number of simulation years N [14]. This is the method used in the developed software as MCS is utilized.

$$LOLE_{MCS} = \frac{\sum_{i=1}^N (\sum_{j=1}^M x_j \cdot \Delta t)}{N} \quad (2.15)$$

An analysis of LOLE and LOLP is typically performed to determine the installed capacity needed to meet a desired reliability value. Such a desired value could be an exemplified LOLE value of 0.1 days/year. The terms LOLP and LOLE are often used interchangeably, as the historical measure was focused on the value of how many days the shortage could be represented by, instead of the total outage time. LOLP is defined as a probability, while LOLE is defined as an expected number of occurrences during a specific period. This is why LOLE is consequently dependent on the time period studied [18, 20].

2.2.3 Loss of Load Frequency

The Loss of Load Frequency (LOLF) is a frequency based index which is given by the number of loss of load events per studied period. In the case of a new system state with a LOL event, the system failure can be counted when the system crosses the boundary between a set of adequate states and a set of LOL states [14, 6]. LOLF is defined by the frequency of *transitions* from LOL states to adequate states, and the commonly used unit is *occurrences/year*. LOLF represents the frequency of system failures and can be expressed mathematically as shown in Equation 2.16 [6].

$$LOLF = \sum_{i \in \mathcal{S}} (F_i - f_i) \quad (2.16)$$

The set of failure states are denoted as \mathcal{S} , while the set of adequate states are defined by their exclusion from \mathcal{S} . F_i denotes the frequency of departing system states i , while f_i denotes the portion of F_i that does not cross the boundary between the set of adequate states and LOL states [14, 21].

Similar to the other reliability indices, LOLF can be expressed for MCS shown in Equation 2.17 [6, 14].

$$LOLF_{MCS} = \frac{\sum_{i=1}^N z_i(x_{i-1}, x_i)}{N}, \quad z_i = \begin{cases} 1 & \text{if } (x_{i-1} = 0) \cap (x_i = 1) \\ 0 & \text{if } (x_{i-1} = 1) \cap (x_i = 1) \\ 0 & \text{if } (x_{i-1} = 1) \cap (x_i = 0) \\ 0 & \text{if } (x_{i-1} = 0) \cap (x_i = 0) \end{cases} \quad (2.17)$$

The variable z_i is summed for all simulation years N , which expresses an average of the variable as result. The variable z_i is 1 if the current state x_i is on outage and it is preceded by an adequate state x_{i-1} . This means that the system failure is only registered if the system state in this time increment has LOL and the previous system state was adequate.

In addition to identifying the expected frequency of load deficiencies in a power system, Loss of Load Duration (LOLD) identifies the expected duration of these deficiencies. Although LOLD is not widely used, it can still give insight on the reliability of a system. The duration index is calculated as shown in Equation 2.18, where the unit is given as [hours/disturbance] [22].

$$LOLD = \frac{LOLE}{LOLF} \quad (2.18)$$

2.2.4 Expected Energy Not Served

Expected Energy Not Served (EENS) is a probabilistic expectation and severity based index. It is also known in HL-1 assessment studies as the indexes Expected Energy Unserved (EEU), Loss of Energy Expected (LOEE) and Expected Unserved Energy (EUE) [15]. EENS is the expected energy amount that is not supplied to the load of the system, due to unexpected power outages, transmission restrictions or capacity deficit [16]. The difference between EENS and LOLE, is that two individual capacity deficits of 10 MW outage and 50 MW outage are treated equally in LOLE calculations if the duration of

these outages are equal, whereas EENS is based on the size of the outage. The reason LOLE is not differentiating these outages is because the same LOLP is yielded in both of these situations. In reality, the outage with a larger energy deficit should be treated as more severe. This is possible with EENS since it includes the size of capacity outages. The expression below in Equation 2.19 shows the EENS at a given time increment for one specific capacity outage, denoted $E_j^{not\ served}$ [19, 15]. Equation 2.19 is only applicable to HL-I studies, as it relies directly on the difference between load and generation capacity without taking the transmission model into account.

$$E_j^{not\ served} = [x_j - (C - L_t)] \cdot P(X = x_j) \quad (2.19)$$

The specific capacity outage is denoted as x_j and L_t is denoted as the given load in the time increment. $[x_j - (C - L_t)]$ is the capacity deficit, which is multiplied with the individual probability of being in the outage state responsible for the capacity deficit $P(X = x_j)$.

Normally a HPL would be used as the load model for EENS, as it gives the sum of all outage states that yield a capacity outage for a given hourly load. The total EENS summed over all hourly loads in a year would therefore be expressed as Equation 2.20 below [15].

$$EENS = \sum_{t=1}^{8760} \sum_{x_j=(C-L_t)}^C [x_j - (C - L_t)] \cdot P(X = x_j) [MWh/year] \quad (2.20)$$

Similar to the previous sub-chapters, the severity based index EENS can be expressed simpler with different parameters. This expression is applicable to HL-II studies as it is not based directly on the difference between load and generation capacity. This mathematical expression is shown below in Equation 2.21 [6].

$$EENS = \sum_{i \in S} p_i \cdot C_i \cdot T \quad (2.21)$$

S is the set of system states with loss of load, p_i is the probability of occurrence of the failure state, and C_i the severity of the energy deficit. T is the evaluation time period, expressed as hours per year to obtain a normal energy quantity.

Similar to the other LOL indices, the analytical method of EENS can be expressed for MCS. By adding the severity of energy deficits C_j to the LOLE expression of Equation 2.15, the calculation of EENS for MCS can be expressed below as Equation 2.22 [6].

$$EENS = \frac{\sum_{i=1}^N (\sum_{j=1}^M x_j \cdot C_j \cdot \Delta t)}{N} \quad (2.22)$$

In the instance without a loss of load event in Equation 2.22, x_j equals to zero, resulting in zero energy deficit.

2.3 Monte Carlo Simulation

As stated in the introduction, the stochastic nature of a power system introduces the need for a modelling system which takes this into account. A common stochastic approach in the field of PSR is the use of Monte Carlo Simulation (MCS). MCS is a tool used for sampling of system states, and is used in this thesis as a way to generate a sequenced set of events, based on data of a system and its components. As its namesake suggests (Monte Carlo being the gambling center of Monaco), MCS utilizes generation of random numbers. Combining this with data of distribution, it produces a model of the system evaluated in the time increments over a given period. MCS is a flexible method and can be utilized in non-sequential and sequential simulation. Both methods will be explained, but this thesis will utilize a non-sequential MCS method due to computational limitations.

The goal of a MCS is to predict and simulate a system's behavior over time in a given environment, based on known or estimated values. As explained in [21], there exist multiple forms of MCS methods. This section of the thesis will focus on the three most commonly used methods; the state sampling, state duration and state transition methods [14, 6, 21]. The basic principals regarding all MCS methods will also be included. The presented MCS methods in the following sub-chapters is based on [21, 6, 18].

2.3.1 MCS Basics

When using MCS in this thesis, the goal is to obtain a history of a system's state vector. The state vector can be represented as

$$\mathbf{S} = [S_1 \quad S_2 \quad \dots \quad S_n]$$

Each element in the state vector denotes the status of a specific component in the system at a given time. In a normal system, the status will be represented by either a "0" or a "1". When a component number i is *Up* (available), it can be represented as $S_i = 0$. If component i is *Down* (unavailable), it can in the same manner be written as $S_i = 1$. The terminology *Up* and *Down* for states of components in a system is commonly used, and will be used throughout this thesis [6, 18]. Four components states in an example system can therefore be expressed in the following manner.

$$\mathbf{S} = [0 \quad 1 \quad 1 \quad 0]$$

Here component one and four is *Up*, while number two and three is *Down*. When a system is derated, the state of a component can be expressed with a value in the scope of [0,1].

MCS is utilized to produce a history of the systems state's in the given time frame, and these states can be used to determine the reliability indices for the system. However it is important to note that non-sequential methods are not able to produce frequency and duration indices, as it does not consider the chronology of the system states.

2.3.2 State Sampling Method

The state sampling method is a non-sequential method. A non-sequential method is a method where the state of the system at any time is independent of the previous state, and the next state will not be affected by the current state [18]. In other words, the method does not operate with a chronological order. This sets it apart from the two other methods in the following subsections.

When applying this method to a system, the FOR of each component is needed. As an example, if one assumes that a given component has a FOR of 25%, the MCS method will generate a random number for each component in the system, ranging between 0 and 1 [18]. If the number for this specific component is smaller than 0.25, the component is *Down*. Otherwise the component is *Up*. For a derated system, the range would be split between the possible states of the component, based on each state's FOR value or derated state probabilities [21]. A component with derated state probabilities $P_{\text{State X}} = 0.25$, $P_{\text{State Y}} = 0.15$ and $P_{\text{Down}} = 0.05$, would be in state X if the random number generated is between 0.25 and 0.15, in state Y if the number is between 0.15 and 0.05, and considered *Down* if the number is smaller than 0.05. For any random number larger than 0.25, the component is evaluated as *Up*.

As previously mentioned, the state sampling is not capable of simulating transition times since it is non-sequential, and is therefore not useful for obtaining frequency and duration indices. To be able to acquire these indices the method used needs to be sequential.

2.3.3 State Duration Method

A commonly used sequential method is the state duration method [6], also referred to as the state duration sampling approach [21]. This method evaluates the duration of each component in the system based on its failure rate and repair rate. By generating random numbers for each individual component, the next change in system state is given, and the data for the duration of each state is recorded.

The failure and repair rates of a power system is often given by an exponential distribution function [21]. This needs to be accounted for, and the common approach is to utilize the inverse transform [6, 18].

Equation 2.23 is an example of how the state duration method would sample a component's time to fail (TTF) or time to repair (TTR), represented as the value T_i . U_i is a randomly generated number in the range $[0,1]$, while λ_i is either the component's failure rate or repair rate (depending on its current state) [21].

$$T_i = \frac{-1}{\lambda_i} \ln(U_i) \quad (2.23)$$

When applying the state duration method, the initial state of the system assumes that all components states is Up . The duration of each component in this state is then sampled by using Equation 2.23, and the component which first changes state, will then define the next state change in the system. The time increment is moved to the next point of state change, and the data for the new state is collected.

To illustrate this method, an example is provided. Table 2.3.1 contains the data for the system, and the code can be found in Appendix B.1. This example follows the steps explained with two generators over a short period of time. This example is not meant to be accurate or typical in regards to a power system, but serves as a visualisation and explanation of the state duration method. Different generation capacities, failure rates and repair rates are chosen. To keep the system's simulation simple, the failure rate and repair rate of each component is kept the same.

Table 2.3.1: Data used in state duration example

Component	Component 1	Component 2
Generation Cap [MW]	15	20
Failure Rate	0.25	0.20
Repair Rate	0.25	0.20

As the results in Table 2.3.2 shows, many time steps can pass without any change of states. There can also occur rapid changes, as it is dependant on the random number generation. Figure 2.3.1 shows that the change in system states of the individual components affect the generation capacity, and that the summation of the component's states in the system is important to be aware of. The lack of a value at time step 25 ($y = 25$), is due to the system not changing states, thus not collecting any new data.

Table 2.3.2: Results of state duration method example

Time [step]	System State [comp 1, comp 2]	Generation Capacity [MW]
0	[0,0]	35
8	[0,1]	15
17	[1,1]	0
22	[1,0]	20
23	[1,1]	0
24	[0,1]	15

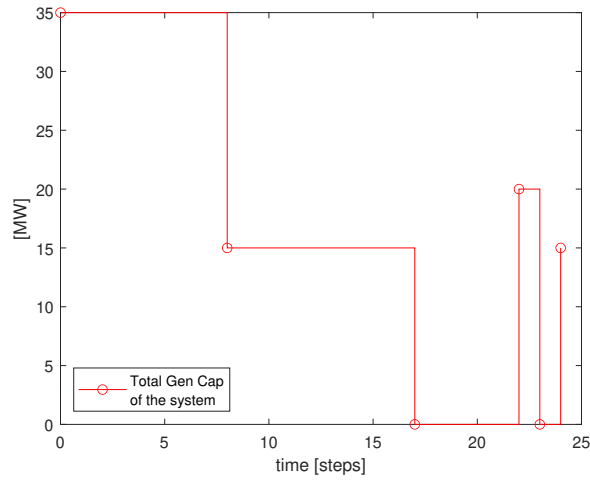


Figure 2.3.1: Total generation capacity during the steps of the state duration method example

Figure 2.3.2 notes any changes in the state of the system with a black circle. As previously noted, a value of 0 represents that the component is *Up* while a value of 1 represents that the component is *Down*. In Figure 2.3.2, it can also be observed that component 1 has fewer changes than its counterpart, despite the fact that it has a higher failure rate. This highlights one of the challenges when designing and computing the state duration method. The simulation needs to run for a significant amount of time to converge on a result. This challenge is further compounded by the need to sample the duration of each component during each iteration of the algorithm [21].

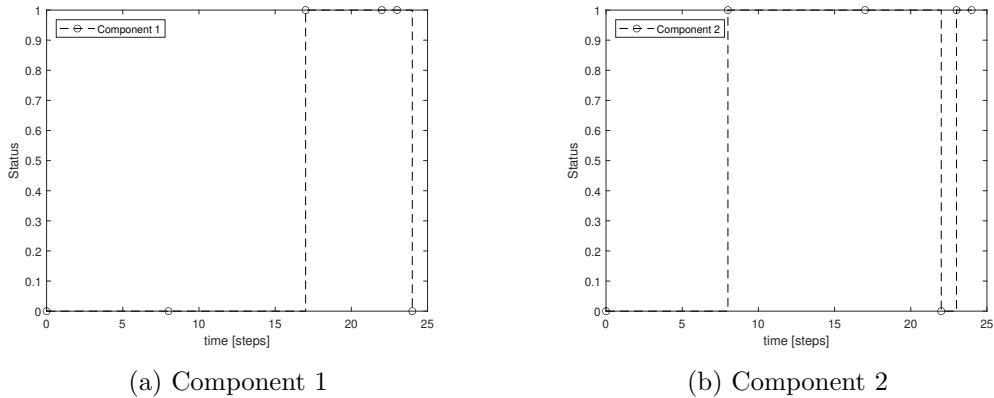


Figure 2.3.2: Example of state duration method, state of the components

2.3.4 State Transition Method

The computational burden involved in the state duration method is improved by the state transition method. Similar to the state duration method presented above, the state transition method is a sequential process. The clearest difference between these two methods, is that while the state duration method evaluates each individual component's time to state transition, the state transmission method evaluates the systems state as a whole. It is important to note that this method only works if all times to transition (both TTF and TTR) are exponentially distributed [6]. As written in [21], it can be proved that if all the components of the system has times to transmissions that is exponentially distributed, the system can be described with a total transmission time T , which shape parameter λ will also be exponentially distributed. λ will be the summation of all individual components' transmission rates from their current state, as shown in Equation 2.24. This method also works for systems with derated components, but this will not be explored further due to the scope of this thesis. The mathematics and proof of this method is further explained and discussed by Billinton and Li [21] in chapter 3.6.3, and is the basis of the presentation of the state transition method in this thesis.

$$\lambda = \sum_{i=1}^n \lambda_i \quad (2.24)$$

Transition of the system from its current state to its next state can be expressed as the shortest transition time between the systems individual components. The shortest transition time is mathematically expressed in Equation 2.25. The lowest value represents the system's departure from its current state [21].

$$\mathbf{T} = \min\{T_1, T_2, \dots, T_n\} \quad (2.25)$$

If it is assumed that the next transition from the current state of the system takes place at instant t_0 . Then the probability that the j th component is the cause of this transition, and its state will be altered by this transition, can be described by Equation 2.26.

$$P_j = (T_j = t_0 | T = t_0) = \frac{P(T_j = t_0 \cap T = t_0)}{P(T = t_0)} \quad (2.26)$$

Equation 2.26 can further be developed to Equation 2.27 [21]. It is evident that the probability of the j th state being the cause of the system's state transition, is the j th state's transition rates from its current state divided by the sum of all components' transition rate from the systems current state [6].

$$P_j = \frac{\lambda_j}{\sum_{i=1}^n \lambda_i} \quad (2.27)$$

Since any system given time and non-zero transition rates must eventually change state, the sum of all the probabilities for state change must be 1, as expressed in Equation 2.28.

$$\sum_{j=1}^n P_j = 1 \quad (2.28)$$

Because of this, it is only necessary to generate one random number in the range $[0,1]$ to decide which component has changed state. This is shown graphically in Figure 2.3.3. $[P_1, \dots, P_m]$ represents the probabilities of each component's change of state, while U is the random number generated. In the case of Figure 2.3.3, the j th component would be the one to change state at the next system state change.

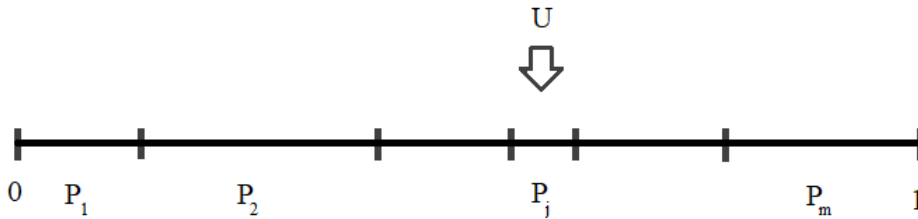


Figure 2.3.3: Visualization of state transition method

To decide when this transition takes place, the generation of an additional number is required. This number, and the system's shape parameter provided by Equation 2.24, is evaluated by Equation 2.23.

Similar to how the state duration method was presented, an example code has been written for the state transition method and can be found in Appendix B.2. The example is based on the same underlying data presented earlier in Table 2.3.1. It is important to mention that this example and its associated code is not a general method, but a specific solution for a system of two components with the included values. It only serves to present and exemplify the method. The simulation runs for 25 time steps, which is undeniably inadequate regarding any degree of precision.

Results for the simulation can be found in Table 2.3.3. It shows that in this case, the number of transitions greatly outnumbers the results of the state duration method, despite being based on the same transition rates. This further illustrates the fact that these methods need to run for a large number of time steps to converge.

Table 2.3.3: Results of state transition method example

Time [step]	System State [comp 1, comp 2]	Generation Capacity [MW]
0	[0,0]	35
5	[1,0]	20
8	[1,1]	0
9	[1,0]	20
10	[1,1]	0
11	[0,1]	15
12	[0,0]	35
15	[1,0]	20
16	[0,0]	35
17	[0,1]	15
21	[1,1]	0
22	[0,1]	15
25	[1,1]	0

In Figure 2.3.4, the total generation capacity of the system can be observed over the time frame of the simulation.

In the same manner as the illustrations in Chapter 2.3.3, the state of the individual components can be found in Figure 2.3.5. Values [0,1] represent states [*Up*,*Down*] respectively, and the black circles denotes the transition times of the entire system.

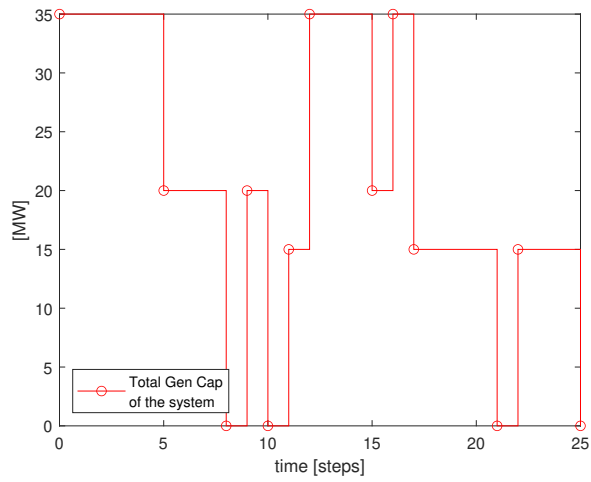


Figure 2.3.4: Total generation capacity during the state duration example

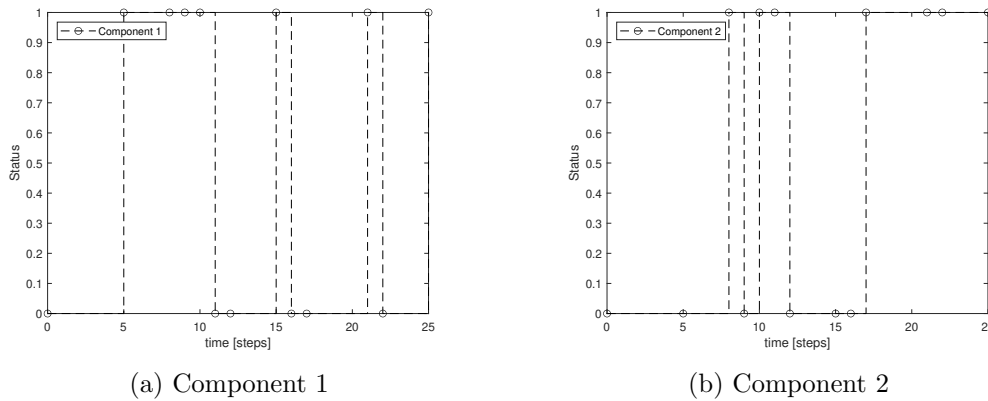


Figure 2.3.5: Example of state transition method, state of the components

As the examples given here are small systems, the different demand of computational power is not shown. However, when the simulated system consists of a larger number of components, the state transition methods reduction of random number generation is impactful [6].

2.4 Capacity Value and Wind Power integration

In this section the concept of capacity value (CV) and wind generation modelling is explored. The focus will be to introduce CV and the different metrics associated with this term. An overview of wind power generation modelling is included, but not explored in depth.

The exploration of CV is important as it is a way to quantify how addition of new generation contributes to the PSR of an existing system. This thesis aims to develop a software (based on the existing work found in [6] and [7]) to quantify the PSR contribution of added wind power generation to an existing system.

For further information on wind generation modelling and how it is integrated into the software, the reader is referred to [7] where both theory and method is explained in detail. As this thesis aims to further develop the software presented in [7], the focus will be on the additions made, not to give an in depth explanation of the software it is based on.

2.4.1 Capacity Value

The reliability indices introduced in 2.2 evaluates a system's current reliability. When new generation is added to an existing system, the system reliability will increase (the indices indicating LOL events or expected energy not supplied will decrease) [13]. The goal of the power system operators and planners is however not always to decrease the risk of power curtailment as much as possible, but to ensure it is kept below a certain threshold. Capacity Value is introduced to calculate how the addition of new generation affects how much the load of this system can be increased.

Capacity Value (CV) represents the contribution to the overall system adequacy for a given generation unit. When looking at a generator, CV signifies the magnitude of load that can be added to the system, while the existing risk level is maintained. When expanding a power system, thereby adding a new generation unit to the system, the load of the system can increase without compromising the generation adequacy. This means that the addition of a generation unit will reduce the risk of power deficit [14, 13, 15, 23, 24].

The traditional adequacy indices lack the ability to express how a resource can meet the reliability conditions of a power system, while improving the system's capability to supply load. This is not possible with the reliability indices LOLE and EENS, as they only evaluate the effect of an added generation unit on the system's reliability level [19, 23]

CV metrics can be estimated by using probabilistic reliability methods, to decompose the generator's contribution to the system reliability. A commonly used metric is the Effective Load Carrying Capability (ELCC), further elaborated below. It is a metric for quantifying the reliability contribution of wind farms and energy storage, and is based on the reliability indices in 2.2.

The ELCC in this report will be estimated based of the adequacy indices LOLE and EENS [14, 13, 15]. It is important to state that ELCC is usually based on LOL-indices. In [19] EENS was tested as a base for ELCC, and to further explore this, both LOLE and EENS will be used (separately) as basis for the ELCC calculations done by the software developed alongside this thesis.

2.4.1.1 Effective Load Carrying Capability

The Effective Load Carrying Capability (ELCC) of a generation plant is a reliability based metric used for evaluating the addition of a conventional or renewable generation plant, by estimating the capacity value. The metric is an established method, first presented by Garver in 1966 [24, 25]. The concept can be explained as follows; the ELCC of an additional generator, is the maximum amount the system load can be increased by after the generator is added, without affecting the system's reliability level. The reliability level is estimated from the loss of load indices. Garver [25] defines ELCC by studying how much the peak load could increase after adding a generation unit, while maintaining the given boundary for generation adequacy. It can be demanding to estimate the load increase based on the peak load, and the definition of ELCC is therefore commonly simplified to cover a constant load instead [24, 26]. This is further explored in Section 3.1.2.

The approach of ELCC calculation utilising LOLE as the benchmark, is presented in the following two formulas below, Equation 2.29 and Equation 2.30. Here LOLE is evaluated by comparing the old existing system to the new system, which are represented with the notation O and N respectively [14, 19, 15]. As Equation 2.30 evaluates the system based on generation and load without including the transmission system, it is only applicable to HL-I studies.

$$LOLE_O = LOLE_N \quad (2.29)$$

$$\sum_{i=1}^n P_i(X_O > C_O - L_i) = \sum_{i=1}^n P_i(X_N > (C_O + C_{gen}) - (L_i + \Delta L)) \quad (2.30)$$

where:

- $LOLE_O$ = LOLE of the old existing system
 $LOLE_N$ = LOLE of the new system
 L_i = Load condition during time increment i [MW]
 ΔL = Additional load that can be served by the new system [MW]
 n = Total number of time increments in the evaluation period
 C_O = Total possible generation capacity of the old existing system
 C_{gen} = Maximum capacity of the generation newly added to the system

The calculation of ELCC can be explained by acknowledging that an existing power system has a specific system reliability index value. This reliability index will improve when a new generator is added to the already existing system. The system will now be able to handle a greater load at the same reliability level as before the addition. The additional load ΔL that can now be supplied because of the addition of a new generator, is the capacity value of the new generator. The system reliability of the new system is equal to that of the old system [13].

For HL-II studies the ELCC of a composite power system can be obtained by iteratively increasing the additional load ΔL until the two values of LOLE are equal. The corresponding ΔL will represent the additional load that the new system can reliably handle, when the extra generation unit with capacity C_{gen} is added. The ΔL that satisfies the condition in Equation 2.29 is quantified as the ELCC for the generation capacity added to the system. ELCC is commonly presented in the unit of [MW], but can also be presented in the unit of [%], as the percentage of the generator's capacity. If the latter is the case, Equation 2.31 expresses the ELCC relative to the capacity of the additional generation unit in Equation [14, 19].

$$ELCC = \frac{\Delta L}{C_{gen}} \times 100\% \quad (2.31)$$

Using EENS instead of LOLE as the basis of ELCC calculations has been tried in [19]. This follows the same methods as explained above, substituting Equation 2.29 with 2.32. This thesis work will incorporate the method presented in [19] and obtain the ELCC based on both the traditional LOLE and the proposed EENS.

$$EENS_O = EENS_N \quad (2.32)$$

- $EENS_O$ = EENS of the old existing system
 $EENS_N$ = EENS of the new system

When calculating the ELCC of a composite power system in HL-II studies, Equation 2.29 or 2.32 is utilized. In this thesis a system is simulated by use of MCS over a period of time. A benchmark load, generation and transmission model is initialized. Each state of the system is subjected to an OPF analysis, and when the simulation has completed, the benchmark reliability indices are calculated. Then the additional generation (wind power generation in this case) is added to the generation model. To obtain the ELCC, the load model is increased and the MCS of the system is run again. The increase in the load model is varied until the resulting reliability index equals that of the benchmark system. This process is further explained in 3.1.

2.4.2 Equivalent Firm Capacity and Equivalent Conventional Capacity

The Equivalent Firm Capacity (EFC) and the Equivalent Conventional Capacity (ECC) are two CV metrics which are based on replacing the added renewable generation with a fictitious conventional generator[19]. The two metrics are quite similar, as the both uses a reliability metric like LOLE to evaluate a system. The generation capacity of the fictitious generator is iteratively increased, until the reliability index chosen equals that of the original system where the renewable generation is present. This is presented in Equation 2.33 and 2.34 [19].

$$LOLE_{goal} = LOLE_{current} \quad (2.33)$$

$$\sum_{i=1}^n P_i(X_{goal} > C_{goal} - L_i) = \sum_{i=1}^n P_i(X_{current} > (C_{goal} + C_{gen}) - L_i) \quad (2.34)$$

where:

$LOLE_{goal}$	= LOLE of the system with additional generation
$LOLE_{current}$	= LOLE of the system with the fictitious generator
L_i	= Load condition during time increment i [MW]
n	= Total number of time increments in the evaluation period
C_{goal}	= Total possible generation capacity of the original system [MW]
$C_{current}$	= Maximum generation capacity of the fictitious generator [MW]
$P_i(X_{goal} > x)$	= The cumulative probability obtained from the original COPT
$P_i(X_{current} > x)$	= The cumulative probability obtained from the new COPT

The difference between ECC and EFC is that the ECC introduces a conventional generator with a related FOR, while the EFC introduces an ideal generator, where the FOR is equal to zero.

The ECC and EFC are useful metrics for quantifying the CV of a system. However the preferred CV metric in PSR studies is ELCC when the different CV metrics is of equivalent value to the study in question [27, 26]. The software developed through this thesis will use the ELCC to quantify the CV of added generation to a existing composite power system.

2.4.3 Wind Generation Modelling

Wind power is one of the fastest growing renewable energy sources, as it is cost-effective and sustainable. Installations of sizable wind power generation results in large-scale integration on the power grid which subsequently results in large power fluctuations, due to the intermittent wind speed. These power fluctuations will pose a risk when trying to provide an adequate generation supply. When there is an unpredictable generation due to intermittent winds and a probabilistic behaviour of turbine outages, it results in a non-schedulable power output. This output is what determines the importance of developing modelling techniques for wind turbine generation. These models can be utilised in reliability evaluation of power systems with integrated wind power [28, 29].

The wind generation modelling can be separated by three steps in the following order:

1. Wind Speed Modelling
2. Wind Generator Modelling
3. Wind Farm Modelling

It should be noted that a wind generation model utilised for a PSR study is interconnected with the methods and considerations used to determine the system model. This is because the choices made when modelling each element will impact the modelling of the other [14, 19].

2.4.3.1 Wind Speed Modelling

The power generated by a wind turbine generator (WTG) is highly dependant on the wind speeds affecting this particular turbine. It is worth remembering that wind power is an intermittent energy source, as the wind speeds will almost constantly fluctuate over time. Because of these unpredictable wind speeds, accurate models are necessary for prediction purposes. There are numerous ways to model the wind speed for PSR studies, where the most common method is modelling in hourly wind speed series. This involves measuring the wind speeds at a certain location in hours over a given time period, and utilizing these measurements to construct an hourly wind speed series [14, 19, 30].

The importance of wind speed is its correlation to the power curve of a wind turbine. A power curve is a graph that indicates the power output of a turbine based on different wind speeds. The wind speed in an area can be obtained by the measured historical data, or from statistical models and simulations. Historical data is based on wind measurements required at the installation site for at least 12 months, measured at different heights [31]. Historic sequences of measured wind speeds have low probability of occurring in the same sequences as when measured, which makes it difficult to predict the wind speed data. This is why utilising the average values of historically measured data can give more accurate prediction [14, 19, 30].

Weibull probability distribution used for the calculation of wind speed samples, is expressed in Equation 2.35. W_s is the wind speed, while α and β are the scale parameter and shape parameter respectively. The scale parameter represents the mean wind speed, while the shape parameter represents the standard deviation of the distribution. The probability function derived by the Weibull distribution will be affected if these parameters are altered [14, 32].

$$f(W_s) = \frac{\beta}{\alpha} \left(\frac{W_s}{\alpha} \right)^{\beta-1} e^{-\left(\frac{W_s}{\alpha}\right)^\beta} \text{ for } \alpha, \beta, W_s \geq 0 \quad (2.35)$$

This can then be transformed to the Weibull cumulative probability function as expressed in Equation 2.36.

$$F(W_s) = 1 - e^{-\left(\frac{W_s}{\alpha}\right)^\beta} \text{ for } \alpha, \beta, W_s \geq 0 \quad (2.36)$$

The wind speed equation can be solved by using the inverse transform method. The values of α and β are determined, and the cumulative probability function $F(W_s)$ is set equal to U , which is a random uniformly distributed number in the range [0,1]. The expression for wind speed can then be expressed as Equation 2.37 [32].

$$W_s = \alpha \left(-\ln(U) \right)^{\frac{1}{\beta}} \quad (2.37)$$

Another possible way of modelling wind speed is by using the Auto-Regressive and Moving Average Model (ARMA). ARMA incorporates the chronological element of wind speed. This is further elaborated in [7], but will not be incorporated in this thesis.

2.4.3.2 Wind Turbine Generator Modelling

The wind turbine output can then be modelled as a function of wind speed, which is simulated by the Weibull distribution function. By passing the hourly wind speeds through a WTG power curve, the hourly power output of a WTG can be obtained. The essential purpose of the WTG power curve is determining the power output for different wind speeds [14, 30, 32].

The power curve shown in Figure 2.4.1 is based on a Vestas V90-2MW turbine, which is a three-bladed horizontal axis wind turbine and a popular installed turbine worldwide [14]. This power curve is only used for illustration purposes, and is not plotted based of any calculations.

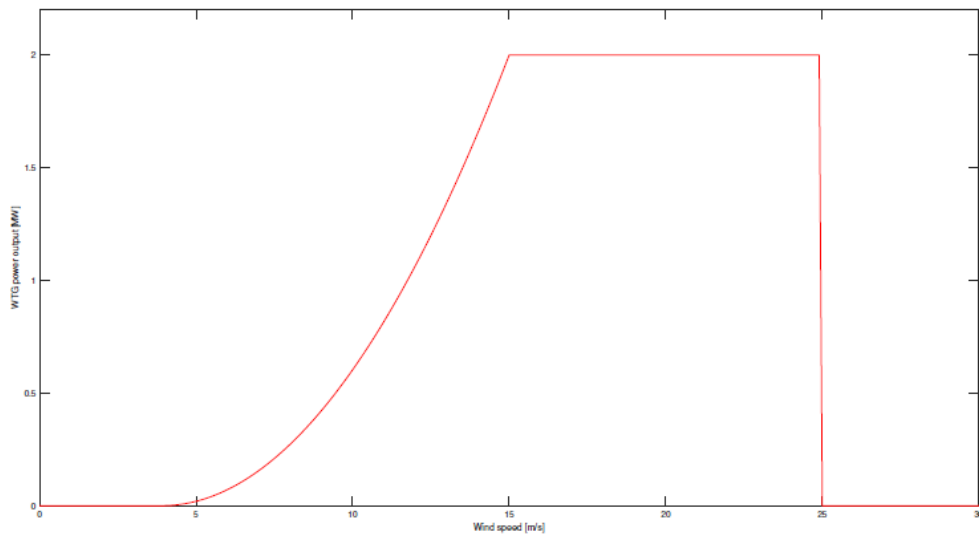


Figure 2.4.1: Power Curve of wind turbine [7]

The power curve in Figure 2.4.1 shows a cut-in speed of 4 m/s and a cut-out speed of 25 m/s. The cut-in speed is when the turbine starts generate to electricity, while cut-out speed is when the turbine shuts off to avoid damage on its equipment due to stress. The rated power output is set for a wind speed of 15 m/s. The power curve shows that when the wind turbine is exposed to velocities higher or lower than the wind speed at rated power, the efficiency decreases.

The wind turbine output that is obtained for the simulated wind speed, $P(W_s)$, is expressed below in Equation 2.38 [32].

$$P(W_s) = \begin{cases} 0 & \text{if } 0 \leq W_s < V_{ci} \\ (A + B \cdot W_s + C \cdot W_s^2) \cdot P_r & \text{if } V_{ci} \leq W_s < V_r \\ P_r & \text{if } V_r \leq W_s < V_{co} \\ 0 & \text{if } W_s \geq V_{co} \end{cases} \quad (2.38)$$

where:

W_s = the wind speed [m/s]

P_r = power output of wind turbine at designed rated speed [MW]

V_{ci} = designed cut-in speed of wind turbine [m/s]

V_r = designed rated speed of wind turbine [m/s]

V_{co} = designed cut-out speed of wind turbine [m/s]

When knowing the parameters given above, the constants A, B and C can be calculated as shown below. When these constants are calculated as functions of V_{ci} and V_r , the calculation of the WTG power output $P(W_s)$ in Equation 2.38 is obtainable.

$$\begin{aligned} A &= \frac{1}{(V_{ci}-V_r)^2} [V_{ci}(V_{ci} + V_r) - 4V_{ci}V_r(\frac{V_{ci}+V_r}{2V_r})^3] \\ B &= \frac{1}{(V_{ci}-V_r)^2} [4(V_{ci} + V_r)(\frac{V_{ci}+V_r}{2V_r})^3 - (3V_{ci} + V_r)] \\ C &= \frac{1}{(V_{ci}-V_r)^2} [2 - 4(\frac{V_{ci}+V_r}{2V_r})^3] \end{aligned}$$

2.4.3.3 Wind Farm Modelling

When the calculations of wind speed and power output modelling is complete, the individual wind turbines can be combined into a wind farm. The wind farm model of this thesis follows a simple procedure, similar to [14]. Neither wake effect or other correlated effects that influence the production between the individual wind turbines are considered [14].

The state of each wind turbine at each time can be determined through the state transition method, previously explained in Chapter 2.3.4. There are two states for every WTG, available or unavailable. For an available WTG, the standard procedure of calculating the individual power output is performed according to Equation 2.38. For unavailable WTG, the individual power output equals to zero. This can be expressed by Equation 2.39, where P_{total}^{wind} is the total power output of WTGs and n is the number of WTGs in the wind farm [14].

$$P_{total}^{wind} = \sum_{j=1}^n WTG_j \cdot P(W_s), \quad WTG_j = \begin{cases} 1 & \text{if } WTG \text{ is available} \\ 0 & \text{if } WTG \text{ is unavailable} \end{cases} \quad (2.39)$$

2.5 Composite systems

As stated in the introduction, this thesis aims to develop software based on the work presented in [6] which was further developed in [7]. The method of obtaining optimal power flow (OPF) calculations used in this thesis has not been changed from this source material. The theory and method of calculating the OPF of a system in HL-II studies will therefore not be explained in depth. To show how the works presented in [6] and [7] is used, the fundamentals on how the method regarding input and output data is however included. A brief explanation on how the software regards situations when parts of the system are isolated is also included. The reader is encouraged to read the in depth explanations provided in [6] and [7] for further explanation and understanding of the underlying method.

2.5.1 Introduction

Composite systems are systems which include the transmission components as well as the load and generation perspectives of the power system assessment. This requires information and data regarding the network topology, impedances and current limits of the lines included in the evaluation [6]. A system evaluated in HL-I will consider the difference in generation and load, while a HL-II study will depend on a load flow analysis, either DC- or AC-based. The simplified DC-based load flow will be less precise than its AC counterpart, but faster to compute. This is a key point when studying simulations on composite systems, as the sheer complexity of the load flow, number of components and time frame needed for an accurate result, requires powerful computational capacities or a long simulation time [21].

The computational demand will affect the comparison and evaluation of the different MCS methods. It is found in [6] that the state transition method is also shown to be faster than the other two methods presented in this project. The state transition method is also able to produce the distribution of indices, while state sampling is not as it is a non-sequential method. The state sampling method is however shown to be more accurate than the state transition method [6]. The fact that the state sampling method is more accurate than the state transition method is because the method converges earlier, and therefore requires fewer iterations to reach the same degree of precision [7].

2.5.2 General Elements

The proposed composite system simulation algorithms presented in [6] requires data input in a specific format. Any simulation of a system in HL-II done by MCS would require the same data provided [21], but the format would be decided by the author of the code. The following tables and interpretation presented is as written in [6], which is the codebase provided for the study in this project. Another possible codebase would be the MECORE computer program developed at the University of Saskatchewan and enhanced at BC Hydro [21, 33].

2.5.2.1 Input Data

Table 2.5.1 will be used as a basis to represent an example of input data, directly collected from [6]. When calculating the AC load flow, the entire table is used. When computing DC load flow, the resistance and shunt susceptance is ignored. When using a non-sequential MCS method, the table can be used as presented. If the MCS method chosen is sequential, the FOR-column would need to be replaced with both failure and repair rates as a sequential method regards the system's states chronologically.

Table 2.5.1: Line input data, State Sampling AC-solver. [6]

Line	Bus	Bus	FOR	Resistance [p.u.]	Reactance [p.u.]	Half of Shunt Susceptance [p.u.]	Current Limit [p.u.]
1	1	2	FOR_1	R_{12}	X_{12}	y_{10}	lim_1
2	2	3	FOR_2	R_{23}	X_{23}	y_{20}	lim_2
n	5	6	FOR_n	R_{56}	X_{56}	y_{50}	lim_n

As in the previous table, Table 2.5.2 is provided as an example of generation input to a composite system simulation. It's specific to an AC-load flow using the state sampling method. For a DC-approach the reactive power of the generators would be ignored. Similar to 2.5.1 for sequential MCS methods, the FOR column would again need to be expanded to incorporate both failure and repair rates [6, 21].

Table 2.5.2: Generator input data, State Sampling AC-solver. [6]

Generator	Capacity [MW]	Bus#	Min Reactive [MVar]	Max Reactive [MVar]	FOR
1	$P_{cap,1}$	N_1	$Qmin_1$	$Qmax_1$	FOR_1
2	$P_{cap,2}$	N_2	$Qmin_2$	$Qmax_2$	FOR_2
n	$P_{cap,n}$	N_n	$Qmin_n$	$Qmax_n$	FOR_n

Table 2.5.3 [6] gives an example of the format and data for the bus input. This table is valid in its current state for all MCS methods. When utilizing DC-load flow, the voltage limits will be ignored. Both solvers will need the cost of load curtailment, as well as the allocation of load for each bus.

Table 2.5.3: Bus specification, AC-solver. [6]

Bus	Share of load	Vmin [p.u.]	Vmax [p.u.]	IEAR [\$/kWh]
1	$Load_1$	$Vmin_1$	$Vmax_1$	$Cost_1$
2	$Load_2$	$Vmin_2$	$Vmax_2$	$Cost_2$
n	$Load_n$	$Vmin_n$	$Vmax_n$	$Cost_n$

2.5.2.2 System State

When representing the state of the system, the notation of states presented in 2.3.1 is continued, where $[Up, Down]$ is written as $[0,1]$, and derated states can be given in the range $[0,1]$. The states of lines and generators is given by individual state vectors, containing all the components of that type. The generation at each bus can further be obtained by combining all generators located at the bus in mention, according to their state given in the generator state vector. By doing this, one can obtain a generation capacity vector with as many elements as there are buses in the system [6].

For a DC approach, this vector would consist of one column, and rows given by number of buses. For the AC method, the vector is expanded to contain the active power, the minimum reactive power and the maximum reactive power capabilities of each bus.

The load requirements at each bus is also needed. This is represented as a vector consisting of the active power load at each bus for the DC-method, while the AC-method requires both active and reactive power and would be represented as a matrix [6].

2.5.3 Isolated buses and contingency solvers

When examining a composite system, outages can occur for lines as well as generators. This can give rise to a problem where buses are isolated from the rest of the system, or parts of the system being "islanded". This occurs when one or more lines are severed, and the resulting system consists of several sub-systems not connected to each other. A load flow algorithm that does not take this possibility into consideration, will not be able to render the solution of the isolated system. This is due to the inclusion of isolated buses in the Ybus representing the system [6].

Algorithms for detection and handling of isolated buses are covered in detail in [6], where different approaches are evaluated and explored. Algorithms detecting and handling isolation of buses, as well as performing a load flow analysis, are given the name "contingency solvers". The steps in a contingency solver is roughly outlined as:

Step 1: If a line is sampled as down, the admittance of the line is set to zero.

Step 2: If a bus is confirmed isolated, the bus and all corresponding elements are removed from the system and solution.

Step 3: Load curtailment is modified based on where in the system the slack bus is located.

When considering a general algorithm for the detection of isolated buses, a wide array of possible configurations must be considered. As shown in [6] when discussing the subject "3.3.1.4 Identification of Isolated Buses", a solution which correctly evaluates a small, simple system might encounter problems when solving a large system where the buses are numbered in no particular sequence. [6] proposes a two-step iterative general algorithm, where the buses are checked and evaluated from both left to right, and right to left. If a certain combination of parameters are met, a bus is marked and the step is repeated with new information. This solution is evaluated to work on any system of lines and buses, but is also slow and contributes to the computational demand of composite system simulation.

Details and explanations of an AC- and DC-contingency solvers, as well as examples and cases, can be found in [6] and [7].

3 Methodological Approach

This thesis aims to develop a method of acquiring the Capacity Credit of a composite power system's integration of wind power generation. Its secondary objective is to explain the method used in a transparent and comprehensible manner, such that further work related to Capacity Credit evaluation on HL-II systems can benefit from this thesis. With this as a guideline, the methodology of the PSR assessment will be presented in this chapter. The main focus will be on the load model, the State Sampling method used to obtain the system indices, the method of assessing the systems potential added load, and the steps to obtain the systems ELCC based on either LOLE or EENS. The method used to determine the power output of the integrated wind park will be included, it will however not be the main focus of this thesis, and the reader is encouraged to read [7] for a more in-depth explanation on this subject. The systems solution to the OPF problem and how islanding of buses is managed will not be included, as [6] developed this method and explains it in great detail. An overview on this method is however presented in 2.5.3

As an overview, the software tools developed in this thesis are based on [6] where the HL-II method of obtaining the reliability indices was developed, and the further additions made in [7] where the integration of wind power was introduced. Further, a tool to obtain the ELCC through use of the bisection method is developed as a part of this thesis work. The tools, explained further in this chapter, are applied to test systems, the IEEE-RTS, RBTS and the MRBTS. The non-sequential State Sampling MCS method is used to obtain the system indices with and without the integration of the wind power generation. The index used as basis for the ELCC calculation with and without the wind power generation are compared (LOLE or EENS), and the load values of the wind power integrated system is modified by using the bisection method. This is done until the chosen index (LOLE or EENS) of the system without wind integration has the same value as the chosen index (LOLE or EENS) of the system where wind power generation is integrated and the load values are modified. This increase in load is defined as the ELCC of the system.

3.1 Load Model

3.1.1 Standard Load Model

The hourly peak load model is the load model utilized in all simulations completed in this thesis. It provides more nuance and variations than its respective counterparts, the daily, weekly and yearly peak load. The estimate is also considered to be less pessimistic and more realistic. For further information, the reader is directed to Section 2.1.5.

As this thesis aims to complete HL-II studies, not only the load at each time increment is needed, but also the distribution of loads throughout the network is necessary. This is obtained through equation 3.40. The base load model is identical to the one presented in [6] and [7].

$$P_{load,i} = HPL \cdot c_i \quad (3.40)$$

Where:

$P_{load,i}$ = The load at bus i at a given hour [MW]

HPL = The hourly peak load of at a given hour [MW]

c_i = The percentage of the systems load that is located at bus i

To calculate the hourly peak load, equation 3.41 is utilized. The weekly, daily and hourly load tables is given in tables 3.1.1, 3.1.2 and 3.1.3. These tables are used when calculating the load distribution for the IEEE-RTS, RBTS and the MRBTS.

This thesis utilizes the same assumptions as [7] when calculating the base load model:

- Each bus will always take the same percentage of the load, no matter the total load level. As a result, c_i is constant for a given bus i.
- The hourly peak load follows a specified distribution, and is equal for every simulation year.

$$HPL_{h,d,w} = YPL \cdot l_w \cdot l_d \cdot l_h \quad (3.41)$$

Where:

$HPL_{h,d,w}$ = Hourly peak load calculated by hourly, daily and weekly percentages [MW]

YPL = Yearly peak load [MW]

l_w = Weekly peak load as a percentage of yearly peak load

l_d = Daily peak load as a percentage of weekly peak load

l_h = Hourly peak load as a percentage of daily peak load

The peak load values associated with the RBTS and IEEE-RTS can be found in Appendix C and Appendix D respectively. The peak load of the MRBTS is identical to that of the MRBTS.

Table 3.1.1: The weekly peak load, used to obtain the load model of the system

Week	WPL [% of YPL]	Week	WPL [% of YPL]	Week	WPL [% of YPL]	Week	WPL [% of YPL]
1	86.2	14	75	27	75.5	40	72.4
2	90	15	72.1	28	81.6	41	74.3
3	87.8	16	80	29	80.1	42	74.4
4	83.4	17	75.4	30	88	43	80
5	88	18	83.7	31	72.2	44	88.1
6	84.1	19	87	32	77.6	45	88.5
7	83.2	20	88	33	80	46	90.9
8	80.6	21	85.6	34	72.9	47	94
9	74	22	81.1	35	72.6	48	89
10	73.7	23	90	36	70.5	49	94.2
11	71.5	24	88.7	37	78	50	97
12	72.7	25	89.6	38	69.5	51	100
13	70.4	26	86.1	39	72.4	52	95.2

Table 3.1.2: The daily peak load, used to obtain the load model of the system

Day	DPL [% of WPL]
Monday	93
Tuesday	100
Wednesday	98
Thursday	96
Friday	94
Saturday	77
Sunday	75

Table 3.1.3: The hourly peak load, used to obtain the load model of the system

Hour	Winter weeks 1-8 & 44-52		Summer weeks 18-30		Spring/Fall weeks 9-17 & 31-43	
	Weekday [% of DPL]	Weekend [% of DPL]	Weekday [% of DPL]	Weekend [% of DPL]	Weekday [% of DPL]	Weekend [% of DPL]
0-1	67	78	64	74	63	75
1-2	63	72	60	70	62	73
2-3	60	68	58	66	60	69
3-4	59	66	56	65	58	66
4-5	59	64	56	64	59	65
5-6	60	65	58	62	65	65
6-7	74	66	64	62	72	68
7-8	86	70	76	66	85	74
8-9	95	80	87	81	95	83
9-10	96	88	95	86	99	89
10-11	96	90	99	91	100	92
11-12	95	91	100	93	99	94
12-13	95	90	99	93	93	91
13-14	95	88	100	92	92	90
14-15	93	87	100	91	90	90
15-16	94	87	97	91	88	86
16-17	99	91	96	92	90	85
17-18	100	100	96	94	92	88
18-19	100	99	93	95	96	92
19-20	96	97	92	95	98	100
20-21	91	94	92	100	96	97
21-22	83	92	93	93	90	95
22-23	73	87	87	88	80	90
23-24	63	81	72	80	70	85

3.1.2 Increasing the load by ΔL

As explained in section 2.4.1.1, when calculating the ELCC of added generation to a composite power system, the load is increased to the point where the reliability index in question equals that of the benchmark system. This section aims to explain how and why this method of increasing the load model is implemented.

When the generational capacity of the system is increased by adding the wind power generation without increasing the load, the reliability of the system will increase (the LOLE and EENS will decrease). To quantify this decrease and assess the reliable power supply of the system in its new state, the ELCC method increases the load across all hours. This is done by adding a constant ΔL to the load model used in the new system. The ΔL is in the first step of the software tools developed in this thesis, defined as 50% of the added max wind power generation capacity, as is shown in equation 3.42. The calculation of the new load model is further shown in equation 3.43. The method used to increase the precision of ΔL is further explained in 3.4, 3.5 and 3.6.

$$\Delta L = c \cdot C_{gen,max} \quad (3.42)$$

Where:

- ΔL = The load to be added to all time increments [MW]
- c = The percentage the load model is increased by
- $C_{gen,max}$ = The peak generating capacity of the added generation [MW]

$$L_{new} = L_{old} + \Delta L \quad (3.43)$$

Where:

- L_{new} = The new load model of the system across all hours [MW]
- L_{old} = The old load model of the system across all hours [MW]
- ΔL = The load to be added to all time increments [MW]

This method of increasing the load model by a flat, constant load is based on [15] and [27], where in the latter the process of calculating ELCC is explained and optimized by the IEEE organisation "Task Force on the Capacity Value of Wind".

Quote [27]:

The load data is then increased by a constant ΔL across all hours using an iterative process, and the LOLE recalculated at each step until the target LOLE is reached.

In this thesis it is postulated that this also applies to EENS.

It is however important to note that there exist some disagreements on the subject regarding flat load increase. The increase in load is in some sources referred to as a percentage of the load of each individual hour [19]. This method is shown in equation 3.44

$$L'_i = L_i \frac{L'_{max}}{L_{max}} \quad (3.44)$$

Where:

- L'_i = Scaled load level [MW]
- L_i = Base case load level [MW]
- L_{max} = Maximum load in the original load series [MW]
- L'_{max} = Maximum load in the new load series [MW]

This might be a valid option when calculating the ELCC as well, but the method used in this thesis is the constant load increase across all hours resulting in ΔL being calculated as shown in equation 3.42. The decision to treat ΔL as a flat addition to the load is made on the basis of the work presented by IEEE as quoted above [27].

3.2 State Sampling

The step-by-step guide introduced here describes the algorithmic approach used to obtain the reliability indices of a composite power system using the State Sampling approach. The method is similar to the method described in [7] with two differences.

- The ARMA model of wind speed sampling is not included in this thesis.
- The State Sampling does not write to a text file, but outputs to the bisection method tool instead.

Besides these two changes, nothing has been changed from the method described in [7], and the explanation of this method is heavily influence by the step-by-step guide described there.

1. Initialization of the script:
 - Loading the parameters of the simulation.
 - Converting values to the per unit system.
 - Calculation of the power curve parameters.
2. Running of the simulation:
 - (a) During each hour in the year, the following steps are computed:
 - i. For each individual component in the system, generate a random uniformly distributed number U in the range $[0, 1]$. Compare this number against the FOR-value of that component to determine whether this component is in a *Up* or *Down* state.
 - ii. If the system is in a *contingency state*, where at least one of the sampled components is in the *Down* state:
 - By using the Weibull distribution, determine the wind speed at the bus where the wind power generation is installed.
 - Determine the available generation at each bus using the state of the generators, WTGs and the wind speed determined in the previous step.
 - Update the OPF problem with the obtained capacity, line states and load curve.
 - Run the OPF solver.
 - If the OPF solver returns a solution where load curtailment is present, denote a failure and the amount of energy curtailed at which bus(es).
 - (b) Return to step 2(a) until the pre-decided number of years has been simulated.

3. Using these results, calculate the reliability indices.
4. Output the indices of the system to the bisection tool.

The flowchart shown in Figure 3.2.1 visualizes the process described above [7]. The chart is colour coded:

- Green: The initialization of the script.
- Black: The state determination part of the script.
- Blue: The main loop of the script. Keeps track of the hour and the year of the simulation.
- Red: The OPF related part of the script.
- Magenta: The calculation of indices and output to the bisection tool.

As in the step-by-step guide, a contingency state is defined by at least one component being in the *Down* state.

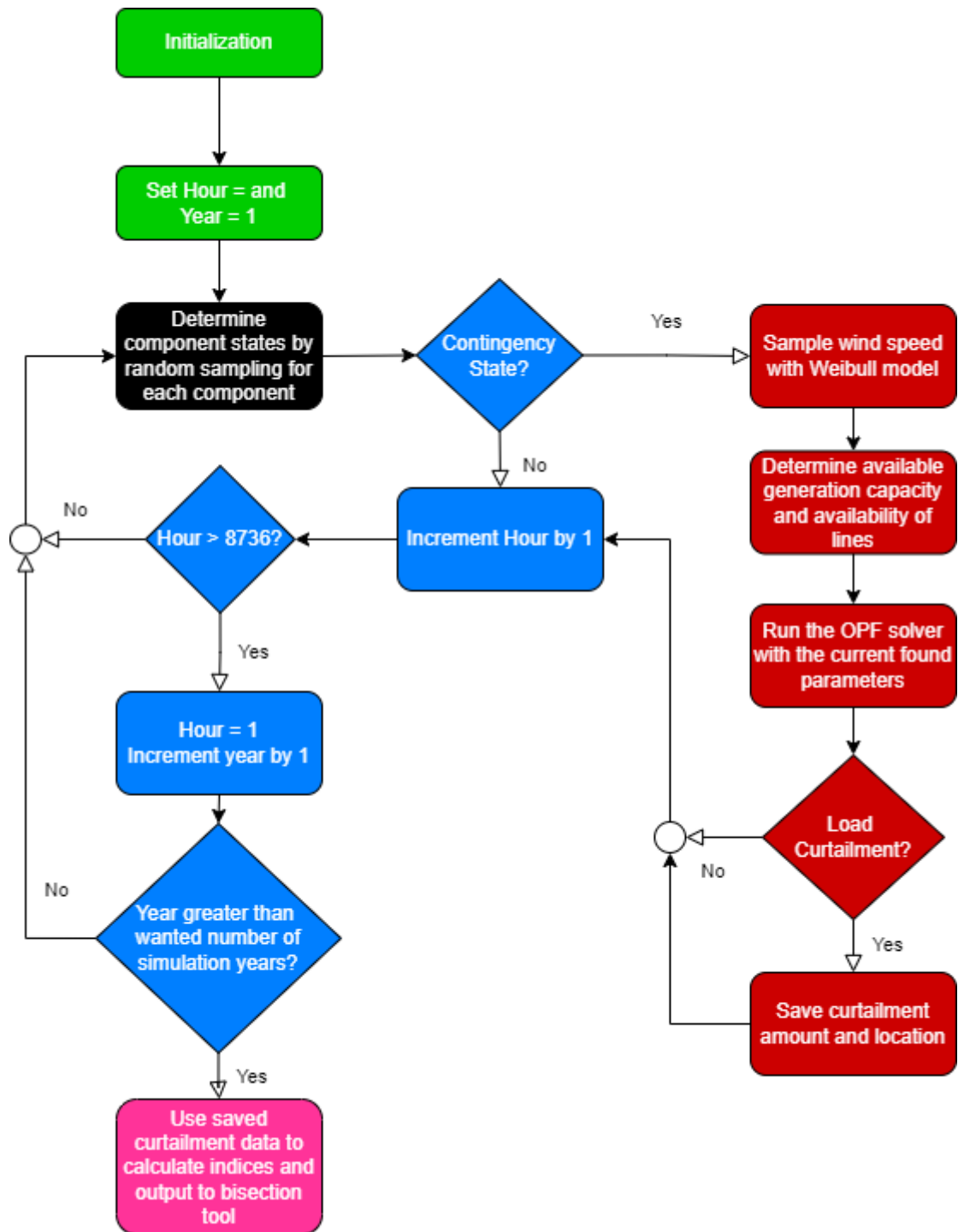


Figure 3.2.1: A flowchart showing how the State Sampling method is used. [7]

3.3 Wind Power Integration

The wind power related data presented here shows an overview of the Wind Turbine Generators (WTGs), how they are connected to the composite power system, and how the wind speed is modelled. The integration of wind power generation to the software developed in [6] is presented in detail in [7], where it first was introduced. For further explanation and details regarding the wind speed modelling and the Weibull parameters used in this thesis, the reader is referred to [7].

The WTGs simulated in this thesis work has a cut-in wind speed of 4 m/s, a rated wind speed of 10 m/s and a cut-out wind speed of 22.222 m/s. Each single WTG is assumed to have a 2 [MW] generation capacity. The FOR of each individual WTG is set to zero.

The WTGs are together considered a Wind Energy Conversion System (WECS) and are connected to the power system with a singular power line. The data for the line is given in Table 3.3.1. In this thesis the WECS is only connected to a single bus in the composite power system. Since wind power generation only is available in one bus, no correlation effects on wind speeds are calculated. Wake effects of WTGs are not considered in this thesis work.

Table 3.3.1: WECS transmission line data [7]

	Unavailability	Average repair time	FOR
WECS transmission line	0.00058	10 [h]	0.0548

The wind speeds utilized in this thesis is the Ørland wind speed model presented in [7]. The wind speed data are presented in Table 3.3.3, and the estimated Weibull parameters of the Ørland wind speed model are presented in Table 3.3.2.

Table 3.3.2: Wind speed data for Ørland [7]

	Ørland [m/s]	Ørland [km/h]
Mean wind speed, μ	7.2274	26.0186
Standard deviation, ρ	3.7366	13.4518

Table 3.3.3: Estimated Weibull parameters for the Ørland wind regime [7]

	Ørland, Trøndelag
α	8.1906
β	2.0604

3.4 Bisection Method

The bisection method is an iterative mathematical tool commonly used for finding the root of a function given two values of the function with opposite signs [34]. This method is also known as the "interval halving method", the "binary search method" or the "dichotomy method". The use of the bisection method is established as a method for approximating the ΔL where the LOLE of the old system equals the LOLE of the new system [35], as shown in equation 2.29. In this thesis it is used to approximate the ΔL where the EENS of the old system equals the EENS of the new system. This is previously explained in Section 2.4.1.1.

The bisection method is defined by two extreme points, where the target value is located in between these. It halves the interval of these extreme points, assesses whether this is the target value, and if not, evaluates in which half the target value can be located [34].

- If the value is located in the higher half, the extreme low point is replaced by the halved interval value.
- If the value is located in the lower half, the extreme high point is replaced by the halved interval value.

The interval between the points is then halved again, and the process repeats until the target value is found.

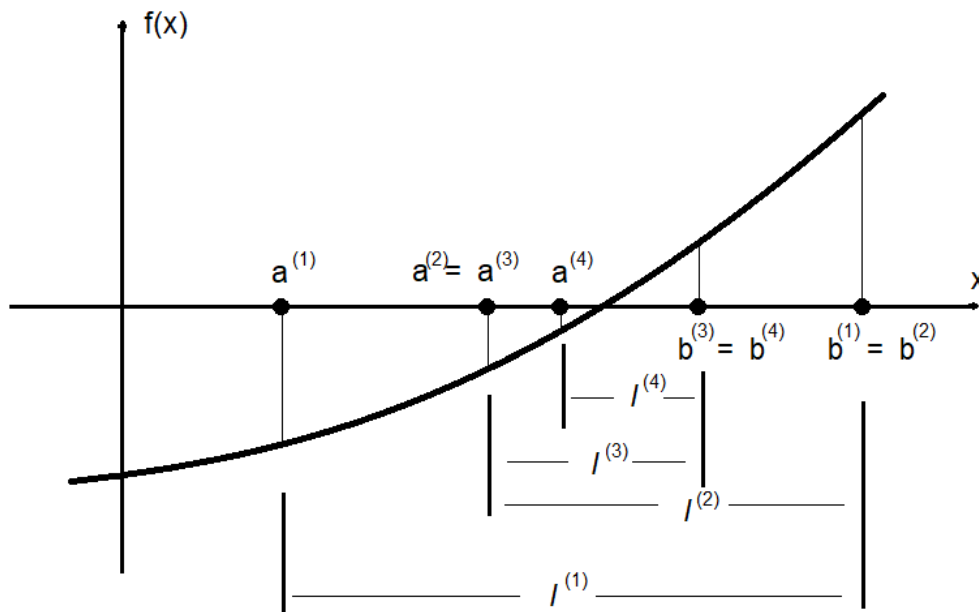


Figure 3.4.1: Illustration of the bisection method [34]

The method is illustrated in figure 3.4.1, where $I^{(1)}$ would be the first interval between the extreme values $a^{(1)}$ and $b^{(1)}$. The interval is halved to $I^{(2)}$ and is not accurate enough to the target value, producing the new extreme low value $a^{(2)}$. As the high value has not changed, $b^{(1)} = b^{(2)}$. The interval is again halved to $I^{(3)}$. Still not accurate enough, this produces a new extreme high value $b^{(3)}$, while the low value is unchanged in this iteration producing $a^{(2)} = a^{(3)}$. This method is iterated until the target value is approximated to be within a defined accuracy interval.

The method is only applicable on continuous functions, and gets more complex if the function is a polynomial [34]. This thesis aims to utilize this method on the reliability/load-curves of the system.

Given the assumptions of the Garver method of approximating the ELCC of a system, the reliability/load-curve can be approximated as an exponential curve [27, 35]. An exponential curve is strictly increasing or decreasing, in this case the risk is growing as the load increases. This determines that the reliability/load-curve is continuous, and that it is ever-increasing. As the complexity of using the bisection method on polynomial functions derives from the functions potential to intersect the line $x = 0$ multiple times, the conditions of the bisection method is met.

The definitions of the extreme values is important for the bisection method to work as it defines the interval in which the reliability index of choice is to be found. The extreme values are the definition of the interval where ΔL exist, and the mean of the extremes is the iterations ΔL . This is shown in equation 3.45.

$$\Delta L_i = \frac{L_{max,i} + L_{min,i}}{2} \quad (3.45)$$

Where:

ΔL_i = The load added to the base load model in iteration i

$L_{max,i}$ = The maximum value of the bisection method in iteration i

$L_{min,i}$ = The minimum value of the bisection method in iteration i

The precision parameter of the analysis decides how precise the LOLE or EENS of the new system needs to be in relation to the benchmark values. This is greatly influenced by the precision of the simulations producing the reliability indices. The number of years the MCS is run is set to 4000 in this thesis and the precision of the ΔL is set to 0.5%. Compared to [7] where the number of years is set to 1000, this number is excessive, but small deviations in the index calculations can result in difficulties for any approximation method to converge. The overall accuracy of the model is hard to determine as it based on both simulation and analytical methods, but through testing it is believed to be approximately 1%.

The steps to the bisection method are as follows.

1. The maximum value of the load increase is first set to 50% of the peak wind power capacity and a MCS of the system is run with ΔL equal to the maximum value. If the reliability index produced by this is lower than the corresponding reliability index of the benchmark simulation, the maximum value is doubled and the simulation is run once more. This repeats until the reliability index produced is higher than the benchmark value. As the reliability/load-curve is strictly increasing, this ensures that the target value is lower or equal to the maximum value.
2. The minimal extreme value of the load increase is set to 0, as the addition of potential generation will only impact the system beneficially. This defines $L_{min,i}$ as the base load model. This ensures that the target value is higher or equal to the minimum value.
3. ΔL is defined by equation 3.45. A simulation is run with this ΔL added to the base load model.
 - (a) If the resulting index is within the precision parameter of the analysis, ΔL is found and the bisection method returns the values of the system with its new values.
 - (b) If the resulting index is lower than the benchmark value, the new maximum value is defined as ΔL . The method returns to step 3.
 - (c) If the resulting index is higher than the benchmark value, the new minimum value is defined as ΔL . The method returns to step 3.

Figure 3.4.2 illustrates how the minimum and maximum values are chosen, represented as L_{min} and L_{max} respectively. The benchmark LOLE is represented as g , and the old and new load curves are illustrated as S_o and S_n respectively. C and D shows the intersection points between the new load curve and the extreme values, and A and B shows the intersection points between the benchmark LOLE and the old and new load curves respectively. L_n shows the load level where the new load curve intersects the benchmark LOLE and the ΔL is defined as the distance between A and B . The ELCC of the added generation is the calculated ΔL .

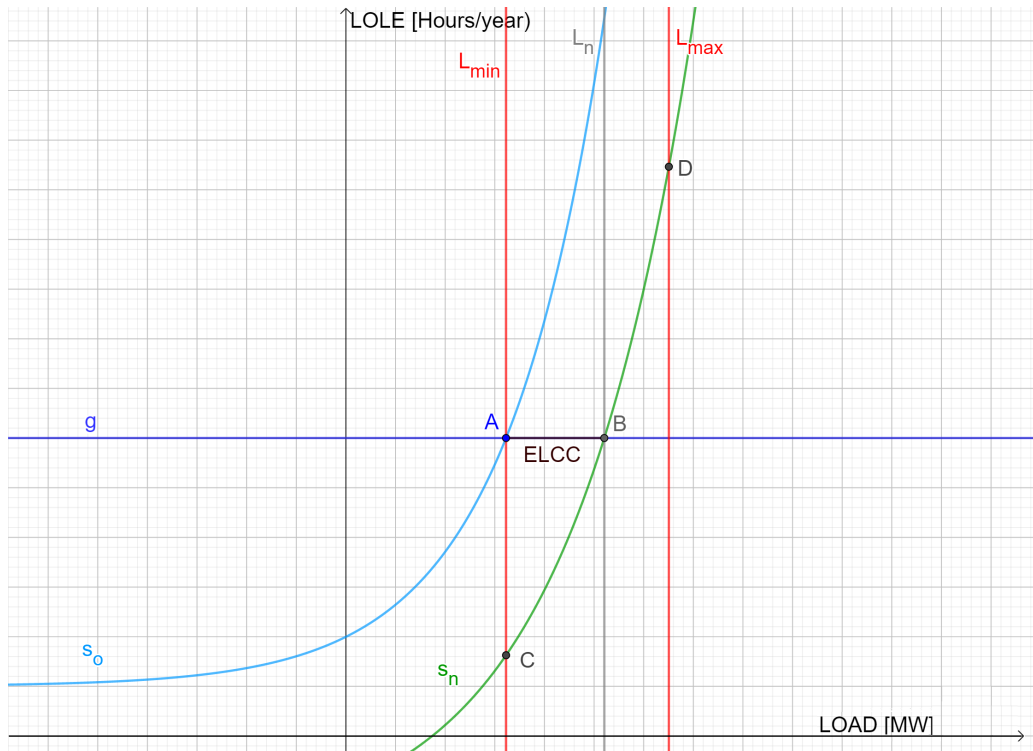


Figure 3.4.2: Example showing the bisection interval of a illustrative system

3.5 ELCC based on LOLE

In Figure 3.4.2, the ELCC of the system is the distance between point *A* and point *B*. The reliability indices of the power system is obtained using the software developed in [6] and [7]. Using the bisection method tool developed through this thesis work, the ELCC of the added wind power generation is approximated for composite systems.

3.6 ELCC based of EENS

If Figure 3.4.2 was drawn for the EENS of the system instead of the LOLE, the distance between point *A* and point *B* would be the ELCC of the system. The method of obtaining the ELCC of the system based on EENS is similar to the method of using LOLE as the basis in every other regard. The concept of basing ELCC on EENS was done in [19] and is further explained in Section 2.4.1.1.

4 Case Studies and Results

This chapter presents the results of the case studies performed with the software developed through this thesis work. The software is applied to the RBTS, MRBTS and RTS. LOLE and EENS is used as a basis for the ELCC calculation and is presented in Sections 4.2 and 4.3 respectively. The data obtained through the ELCC calculations will be presented in a system-by-system order. The ELCC values obtained from each system will be summarised in Tables 4.2.7 and 4.3.7, and discussed in Sections 4.2.4 and 4.3.4, referring to the LOLE and EENS basis of ELCC respectively. All test systems are evaluated in HL-II, where the transmission models of the individual systems are included.

The tables displaying the LOLE and EENS values of the test systems and the "WL-systems" refers to specific versions of the composite systems. The test system written as RBTS, MRBTS and RTS, is the system in its original version, no wind power generation is integrated and the load is not increased. The "WL-systems", written as RBTS-WL, MRBTS-WL and RTS-WL, are the systems in their modified version. In these systems, wind power generation is integrated, and the load has been increased to the point where the reliability index used as basis for the ELCC calculations equals that of the "Benchmark System". For all "WL-systems", the system version satisfies Equation 2.29 or 2.32 depending on which reliability index is used as the ELCC basis. In this thesis, the "WL-systems" is decided to satisfy the conditions of these equations if the index in question is within 0.5% of the corresponding benchmark index.

Detailed information on the RBTS and RTS can be found in Appendix C and Appendix D. The systems presented there have no wind power generation integrated and corresponds to the benchmark values presented in this chapter. The MRBTS is presented in Section 4.1.

Wind power is added to the systems where ELCC is calculated. In the RBTS and MRBTS a wind power plant with 20 [MW] peak generation capacity is added to bus 4. In the RTS a wind power plant with 600 [MW] peak generation capacity is added to bus 19.

Each simulation to produce the reliability indices is run for 4000 years. The required precision of the bisection method is set to 0.5 %.

The time needed to run these simulations vary depending on test system size and computation power available. Obtaining the ELCC of wind power generation added to the RTS averages at approximately 75000 seconds (20+ hours). Obtaining the ELCC of wind power generation added to the RBTS and MRBTS averages at approximately 50000 seconds (13+ hours). Computation efficiency and optimization has not been examined as a part of this thesis work.

4.1 MRBTS

The RBTS presented in Appendix C is a 6-bus system with a designed weakness, the radial connection between Bus 5 and Bus 6 [7, 36]. This weakness can be amended by connecting a secondary transmission line between Bus 5 and Bus 6. This line is designated as Line 10, and has the same parameters as the existing Line 9 connecting Bus 5 and Bus 6. By increasing the reliability of the transmission model, the CV of the system can be illustrated from a different perspective. The modified RBTS, designated as the MRBTS is illustrated in Figure 4.1.1 [7].

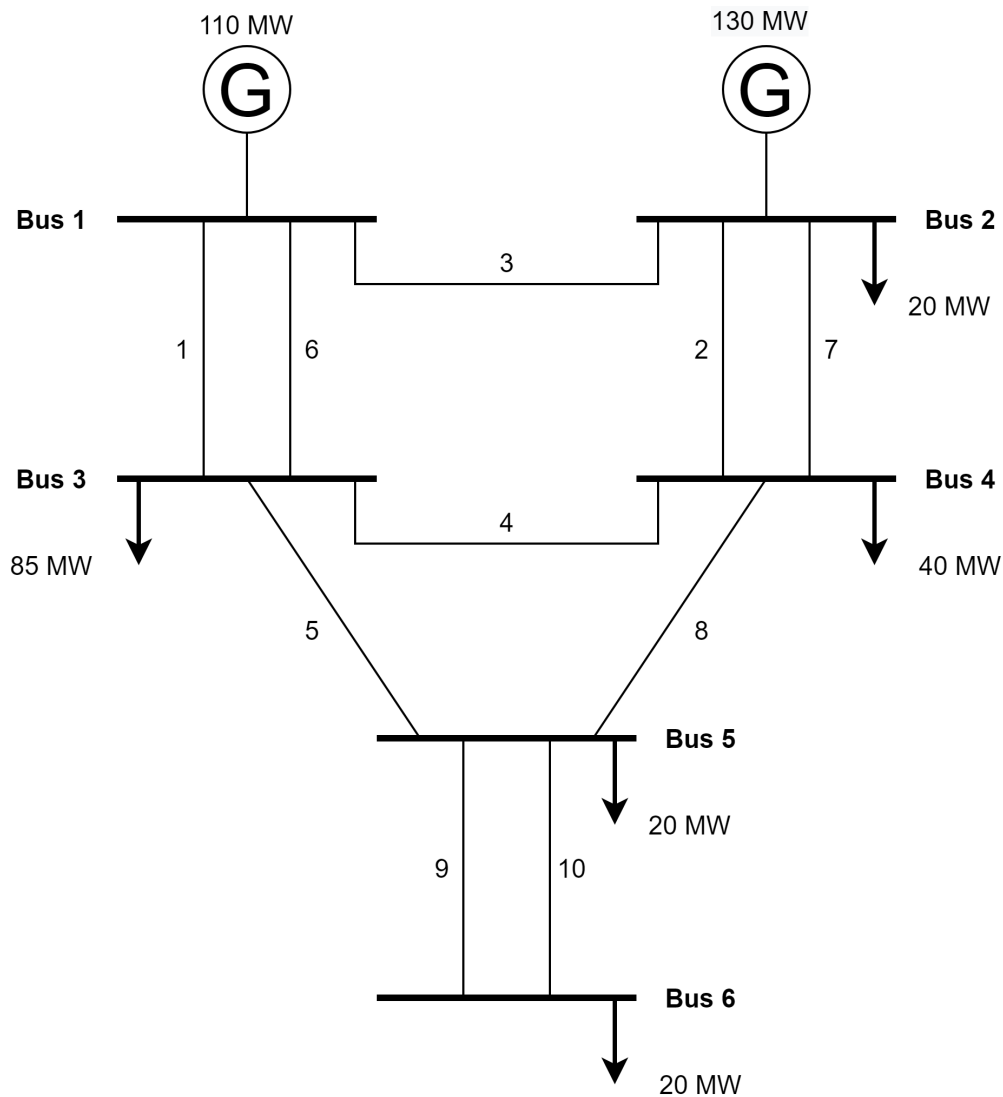


Figure 4.1.1: Single line diagram of the MRBTS [7]

4.2 Obtaining the CV of test systems using LOLE as basis for ELCC calculations

The results presented in this section utilizes LOLE as the basis for determining the ELCC of added wind power generation. To reasonably satisfy the conditions of equation 2.29, the precision of the bisection method is set to 0.5%. Each calculation of the reliability indices is done by the State Sampling Method, which is run for 4000 years.

4.2.1 RBTS

A WECS consisting of 10 WTGs is connected to bus 4 in the RBTS. The WTGs have a cut-in wind speed of 4 m/s, a rated wind speed of 10 m/s and a cut-out wind speed of 22.222 m/s. Each single WTG is assumed to have a 2 [MW] peak generation capacity. The WECS consisting of 10 WTGs has therefore a total of 20 [MW] peak generation capacity. The FOR of each individual WTG is set to zero. The transmission line connecting the WECS to the RBTS has a FOR of 0.0548.

A comparison between the benchmark RBTS and the RBTS-WL is presented in Table 4.2.1. The $ELCC_{LOLE}$ of the added wind power generation to the RBTS is presented in Table 4.2.2 as a added load capacity in [MW] and as a percentage of the installed peak generation capacity. The individual bus indices and the standard deviation for the RBTS-WL can be found in Appendix E.1. The coefficients of variation of the LOLE and EENS for both the RBTS and the RBTS-WL can be found in Appendix G.1.

Table 4.2.1: Comparison of LOLE and EENS between the RBTS and the RBTS-WL when ELCC is based on LOLE

	LOLE	EENS
RBTS	11.1445	133.5532
RBTS-WL	11.1870	140.5018

Table 4.2.2: The $ELCC_{LOLE}$ of added wind power generation integrated in the RBTS-WL

Test System	$ELCC_{LOLE}$ [MW]	$ELCC_{LOLE}$ [%]
RBTS-WL	6.250	31.250

4.2.2 MRBTS

A WECS consisting of 10 WTGs is connected to bus 4 in the MRBTS. The WTGs have a cut-in wind speed of 4 m/s, a rated wind speed of 10 m/s and a cut-out wind speed of 22.222 m/s. Each single WTG is assumed to have a 2 [MW] peak generation capacity. The WECS consisting of 10 WTGs has therefore a total of 20 [MW] peak generation capacity. The FOR of each individual WTG is set to zero. The transmission line connecting the WECS to the MRBTS has a FOR of 0.0548.

A comparison between the benchmark MRBTS and the MRBTS-WL is presented in Table 4.2.3. The $ELCC_{LOLE}$ of the added wind power generation to the MRBTS is presented in Table 4.2.4 as a added load capacity in [MW] and as a percentage of the installed peak generation capacity. The individual bus indices and the standard deviation for the MRBTS-WL can be found in Appendix E.2. The coefficients of variation of the LOLE and EENS for both the MRBTS and the MRBTS-WL can be found in Appendix G.2.

Table 4.2.3: Comparison of LOLE and EENS between the MRBTS and the MRBTS-WL when ELCC is based on LOLE

	LOLE	EENS
MRBTS	1.1295	10.4644
MRBTS-WL	1.1287	10.1357

Table 4.2.4: The $ELCC_{LOLE}$ of added wind power generation integrated in the MRBTS-WL

Test System	$ELCC_{LOLE}$ [MW]	$ELCC_{LOLE}$ [%]
MRBTS-WL	5.332	26.660

4.2.3 RTS

A WECS consisting of 300 WTGs is connected to bus 19 in the RTS. The WTGs have a cut-in wind speed of 4 m/s, a rated wind speed of 10 m/s and a cut-out wind speed of 22.222 m/s. Each single WTG is assumed to have a 2 [MW] peak generation capacity. The WECS consisting of 300 WTGs has therefore a total of 600 [MW] peak generation capacity. The FOR of each individual WTG is set to zero. The transmission line connecting the WECS to the RTS has a FOR of 0.0548.

A comparison between the benchmark RTS and the RTS-WL is presented in Table 4.2.5. The $ELCC_{LOLE}$ of the added wind power generation to the RTS is presented in Table 4.2.6 as a added load capacity in [MW] and as a percentage of the installed peak generation capacity. The individual bus indices and the standard deviation for the RTS-WL can be found in Appendix E.3. The coefficients of variation of the LOLE and EENS for both the RTS and the RTS-WL can be found in Appendix G.3.

Table 4.2.5: Comparison of LOLE and EENS between the RTS and the RTS-WL when ELCC is based on LOLE

	LOLE	EENS
RTS	12.4315	1416.1327
RTS-WL	12.4085	1402.4519

Table 4.2.6: The $ELCC_{LOLE}$ of added wind power generation integrated in the RTS-WL

Test System	$ELCC_{LOLE}$ [MW]	$ELCC_{LOLE}$ [%]
RTS-WL	225.000	37.500

4.2.4 Summation and discussion of results where LOLE is used as basis for ELCC calculations

In Table 4.2.7 the $ELCC_{LOLE}$ of the added wind generation capacity for each test system is presented. Table 4.2.7 shows both the amount the load can be increased by while retaining the benchmark reliability, and the percentage of the installed peak wind generation capacity this represents. This percentage of installed peak wind generation capacity is also presented in Figure 4.2.1.

Table 4.2.7: Summation of $ELCC_{LOLE}$ calculations applied to the different test systems

Test System	$ELCC_{LOLE}$ [MW]	$ELCC_{LOLE}$ [%]
RBTS-WL	6.250	31.250
MRBTS-WL	5.332	26.660
RTS-WL	225.000	37.500

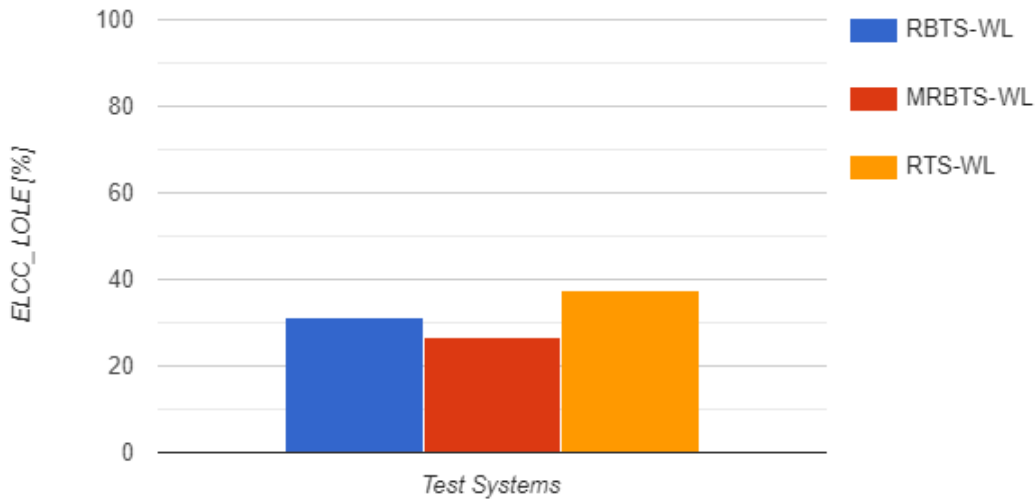


Figure 4.2.1: Bar chart comparing the $ELCC_{LOLE}$ [%] of the test systems.

The $ELCC_{LOLE}$ as a percentage of peak wind generation capacity is largest in the RTS-WL, smallest in the MRBTS-WL and the RBTS-WL is between the two other test systems. The RTS is a system with robust transmission, but lacking generation capacity. This might be why the $ELCC_{LOLE}$ [%] is significantly larger for this test system compared to the others. The installed wind generation capacity in the RTS-WL also constitutes a smaller share of the systems total peak generation capacity, approximately 5.7 %, compared to the RBTS-WL and MRBTS-WL where the installed wind generation capacity constitutes approximately 12 % of the total peak generation capacity. The combination of the ability to transfer the added wind power generation to where it is need, and the relative size of the installation, might explain the relatively large $ELCC_{LOLE}$ [%] found in the RTS-WL.

There are two interesting differences between the results of the RBTS-WL and MRBTS-WL which will be explored here.

- When the LOLE is used as the basis of obtaining ELCC, the EENS of the RBTS-WL increases compared to its benchmark value, while the EENS of the MRBTS-WL decreases.
- The $ELCC_{LOLE}$ of the RBTS-WL is larger than the MRBTS-WL where the transmission system is improved.

When the transmission system of the RBTS is improved, resulting in the MRBTS, the benchmark reliability indices of the system improve significantly, as both LOLE and EENS decreases by approximately a factor of 10 or more (a decrease in the reliability indices constitutes an improvement on the systems reliability). This can be seen in Tables 4.2.1 and 4.2.3. A possible reason for the higher $ELCC_{LOLE}$ values of the RBTS-WL compared to the MRBTS-WL might be the inability of LOLE to assess the magnitude of a LOL-event. As shown in Table 4.2.1, when the LOLE of RBTS-WL equals that of the RBTS benchmark, the EENS of the RBTS-WL is significantly larger than its benchmark counterpart. When examining Table 4.2.3, one can see that this is not the case for the MRBTS-WL, as the EENS of the system decreases between the benchmark system and the MRBTS-WL. As LOLE treats all LOL-events as an equal failure to supply load, the relatively large LOL-events when the radial connection between Bus 5 and Bus 6 is severed is not distinguished from a minor load curtailment. This might explain the difference seen in the EENS values of the RBTS-WL and the MRBTS-WL. It also exemplifies the shortcomings of using only LOLE as a basis of ELCC calculation.

The difference in $ELCC_{LOLE}$ between the RBTS-WL and the MRBTS-WL might be due to the MRBTS being a more reliable system than the RBTS. When the LOLE and EENS benchmark value improves (decreases) as seen in Table 4.2.3, it is due to the composite power system improving. Since the RBTS is a system considered to have a weak transmission system but a comparatively strong generation system, improving the generation system further might result in diminishing returns. The ELCC calculations considers the baseline reliability indices produced for the MRBTS, and by trying to improve on a already reliable system, there is less to gain compared to the RBTS.

4.3 Obtaining the CV of test systems using EENS as basis for ELCC calculations

The results presented in this section utilizes EENS as the basis for determining the ELCC of added wind power generation. To reasonably satisfy the conditions of equation 2.32, the precision of the bisection method is set to 0.5%. Each calculation of the reliability indices is done by the State Sampling Method, which is run for 4000 years.

4.3.1 RBTS

A WECS consisting of 10 WTGs is connected to bus 4 in the RBTS. The WTGs have a cut-in wind speed of 4 m/s, a rated wind speed of 10 m/s and a cut-out wind speed of 22.222 m/s. Each single WTG is assumed to have a 2 [MW] peak generation capacity. The WECS consisting of 10 WTGs has therefore a total of 20 [MW] peak generation capacity. The FOR of each individual WTG is set to zero. The transmission line connecting the WECS to the RBTS has a FOR of 0.0548.

A comparison between the benchmark RBTS and the RBTS-WL is presented in Table 4.3.1. The $ELCC_{EENS}$ of the added wind power generation to the RBTS is presented in Table 4.3.2 as a added load capacity in [MW] and as a percentage of the installed peak generation capacity. The individual bus indices and the standard deviation for the RBTS-WL can be found in Appendix F.1. The coefficients of variation of the LOLE and EENS for both the RBTS and the RBTS-WL can be found in Appendix H.1.

Table 4.3.1: Comparison of LOLE and EENS between the RBTS and the RBTS-WL when ELCC is based on EENS

	LOLE	EENS
RBTS	11.0765	132.7733
RBTS-WL	10.7882	132.6272

Table 4.3.2: The $ELCC_{EENS}$ of added wind power generation integrated in the RBTS-WL

Test System	$ELCC_{EENS}$ [MW]	$ELCC_{EENS}$ [%]
RBTS-WL	2.500	12.500

4.3.2 MRBTS

A WECS consisting of 10 WTGs is connected to bus 4 in the MRBTS. The WTGs have a cut-in wind speed of 4 m/s, a rated wind speed of 10 m/s and a cut-out wind speed of 22.222 m/s. Each single WTG is assumed to have a 2 [MW] peak generation capacity. The WECS consisting of 10 WTGs has therefore a total of 20 [MW] peak generation capacity. The FOR of each individual WTG is set to zero. The transmission line connecting the WECS to the MRBTS has a FOR of 0.0548.

A comparison between the benchmark MRBTS and the MRBTS-WL is presented in Table 4.3.3. The $ELCC_{EENS}$ of the added wind power generation to the MRBTS is presented in Table 4.3.4 as a added load capacity in [MW] and as a percentage of the installed peak generation capacity. The individual bus indices and the standard deviation for the MRBTS-WL can be found in Appendix F.2. The coefficients of variation of the LOLE and EENS for both the MRBTS and the MRBTS-WL can be found in Appendix H.2.

Table 4.3.3: Comparison of LOLE and EENS between the MRBTS and the MRBTS-WL when ELCC is based on EENS

	LOLE	EENS
MRBTS	1.1547	10.7460
MRBTS-WL	1.1513	10.7316

Table 4.3.4: The $ELCC_{EENS}$ of added wind power generation integrated in the MRBTS-WL

Test System	$ELCC_{EENS}$ [MW]	$ELCC_{EENS}$ [%]
MRBTS-WL	5.615	28.076

4.3.3 RTS

A WECS consisting of 300 WTGs is connected to bus 19 in the RTS. The WTGs have a cut-in wind speed of 4 m/s, a rated wind speed of 10 m/s and a cut-out wind speed of 22.222 m/s. Each single WTG is assumed to have a 2 [MW] peak generation capacity. The WECS consisting of 300 WTGs has therefore a total of 600 [MW] peak generation capacity. The FOR of each individual WTG is set to zero. The transmission line connecting the WECS to the RTS has a FOR of 0.0548.

A comparison between the benchmark RTS and the RTS-WL is presented in Table 4.3.5. The $ELCC_{EENS}$ of the added wind power generation to the RTS is presented in Table 4.3.6 as a added load capacity in [MW] and as a percentage of the installed peak generation capacity. The individual bus indices and the standard deviation for the RTS-WL can be found in Appendix F.3. The coefficients of variation of the LOLE and EENS for both the RTS and the RTS-WL can be found in Appendix H.3.

Table 4.3.5: Comparison of LOLE and EENS between the RTS and the RTS-WL when ELCC is based on EENS

	LOLE	EENS
RTS	12.4235	1420.4682
RTS-WL	12.5823	1426.7016

Table 4.3.6: The $ELCC_{EENS}$ of added wind power generation integrated in the RTS-19

Test System	$ELCC_{EENS}$ [MW]	$ELCC_{EENS}$ [%]
RTS-WL	281.25	46.875

4.3.4 Summation and discussion of results where EENS is used as basis for ELCC calculations

In Table 4.3.7 the $ELCC_{EENS}$ of the added wind generation capacity for each test system is presented. Table 4.3.7 shows both the amount the load can be increased by while retaining the benchmark reliability, and the percentage of the installed peak wind generation capacity this represents. This percentage of installed peak wind generation capacity is also presented in Figure 4.3.1.

Table 4.3.7: Summation of $ELCC_{EENS}$ calculations applied to the different test systems

Test System	$ELCC_{EENS}$ [MW]	$ELCC_{EENS}$ [%]
RBTS-WL	2.500	12.500
MRBTS-WL	5.615	28.076
RTS-WL	281.25	46.875

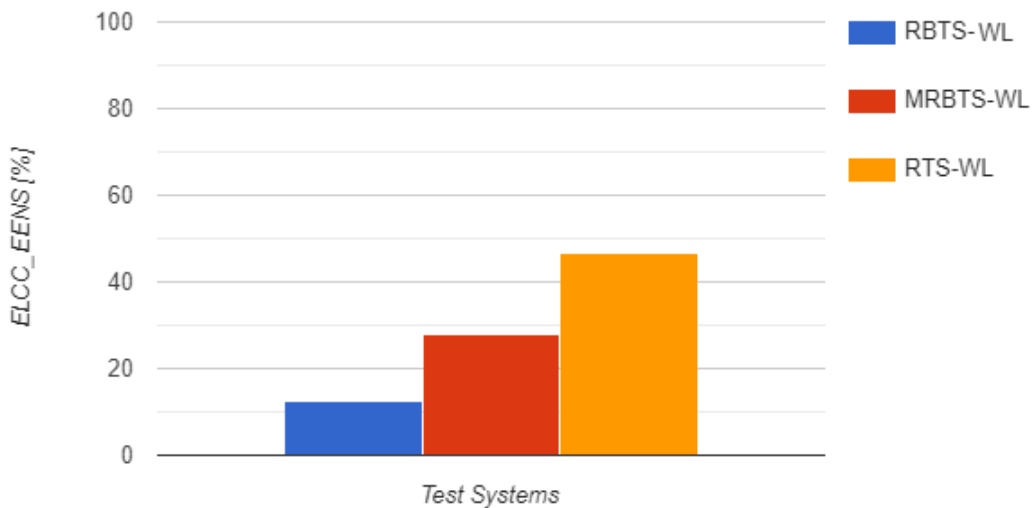


Figure 4.3.1: Bar chart comparing the $ELCC_{EENS}$ [%] of the test systems.

The $ELCC_{EENS}$ as a percentage of the installed capacity is largest for the RTS-WL, smallest for the RBTS-WL and the MRBTS-WL is located between the two other systems. When comparing the $ELCC_{EENS}$ [%] of different test systems it is important to note that the transmission network of the model is very important. EENS is indifferent to the number of LOL-events, but only regards the amount of load not supplied. Therefore the power generated by the WECS and the ability to transfer it to where it is needed is instrumental in determining the $ELCC_{EENS}$ of the composite power system.

Since the RBTS is designed with only a radial connection designated Line 9 between Bus 5 and Bus 6, a fault in this line would render Bus 6 isolated and the system completely unable to supply power this bus. This would result in a large EENS, and the addition of wind power generation in the RBTS-WL would not improve on this aspect of the power system. This explains the relative low $ELCC_{EENS}$ presented in Table 4.3.7 and Figure 4.3.1.

The MRBTS improves the radial connection between Bus 6 and rest of the power system by adding a transmission line between Bus 5 and Bus 6. Information on the MRBTS is presented in Section 4.1. The MRBTS-WL uses this improvement on the systems transmission model to more effectively use the wind power supplied by the WECS. This results in a more than doubling of the $ELCC_{EENS}$ of the MRBTS-WL compared to the RBTS-WL.

The RTS is as stated in Section 4.2.4 a test system with a robust transmission network. This transmission network effectively transfers power to the location in the system where it is needed. This holds true for the RTS-WL, where the $ELCC_{EENS}$ is larger than the $ELCC_{LOLE}$. EENS is not based on LOL-events, but instead the amount of power not supplied. The power generated by the WTGs is therefore in some cases used to mitigate the amount of power the system is unable to supply while not being able to avoid a LOL-event. This improves the $ELCC_{EENS}$ of the system, explaining the difference between the $ELCC_{EENS}$ and $ELCC_{LOLE}$ of the RTS-WL.

4.4 Comparison of LOLE and EENS used as a basis for ELCC

The presented results show that the $ELCC_{LOLE}$ and $ELCC_{EENS}$ present different perspectives on the CV of the added wind power generation. The $ELCC_{LOLE}$ quantifies the added generation based on its ability to stop LOL-events from occurring. The $ELCC_{EENS}$ quantifies the added generation based on its ability to mitigate the amount of load curtailed needed. Both perspectives are valuable, and in combination they produce a more complete CV evaluation of the added generation.

5 Conclusions and Future Work

5.1 Conclusions

This thesis has examined methods of assessing the reliability and Capacity Value of wind power generation integrated in composite power systems. A framework for evaluating the reliability and CV of a composite power system has been constructed through the use of the State Sampling MCS method and the Bisection method. Through a literature review, a methodology suited to the PSR assessment was determined. In-house software tools were developed to evaluate the reliability indices and CV of a composite power system in this HL-II study. This developed software tool was used on the RBTS, MRBTS and RTS.

The literature review was written to give a comprehensive explanation of PSR-studies. Capacity Value was introduced as a method of quantifying generation capacity added to an existing system. The fundamentals of composite system modelling and wind power modelling were presented. The literature study was written to convey information in a clear and concise manner, with the intention of being a viable tool for further use in the ongoing PSR project at the Department of Electrical Power Engineering at NTNU.

Both non-sequential and sequential MCS methods were introduced as part of the literature review. The differences between the State Sampling, State Duration and State Transition method were explained. The State Sampling MCS method was chosen for the case studies due to its relative low number of simulation years needed to converge compared to the other two methods.

The methodology explaining the bisection method and how the load of the system was changed was presented. The load variation needed to calculate the ELCC of the composite power system was determined to be based on flat load variations. The bisection method was illustrated and the precision parameter of the bisection method was introduced. Through the case studies the precision parameter for the bisection method was found to be acceptable at 0.5 %, as this was in general considered to result in a precision satisfying the purpose of this thesis.

Computational efficiency, precision and accuracy of the MCS and DC load flow analysis has not been explored in this thesis. The goal of this thesis has been to develop software tools which were able to quantify the CV of wind power generation added to a composite power system. The State Sampling method was restricted to 4000 simulation years. The resulting reliability indices were considered reasonably accurate, and allowed the bisection method to converge.

The traditional method of basing the ELCC metric on LOLE was compared to the postulated method of using EENS as the basis for ELCC calculation. Differences in the resulting ELCC values were found and discussed. Using EENS as a basis for ELCC gave a new perspective to the CV evaluation of the added generation, and might in some cases be valuable when considering different options for power system expansion.

5.2 Future Work

The CV assessment of wind power integration could be extended to include energy storage, such as Battery Energy Storage Systems (BESS). The possibility of storing power could improve the efficiency of the WESC.

In this thesis the bisection method is used to determine where on the load curve the ΔL is located. The secant method is a possible alternative to the bisection method and could result in reducing the number of reliability indices the script needs to converge on the ELCC.

The integration of solar power to the existing software tools could be of interest. The interaction between solar and wind power production could be explored, and be included in a reliability assessment.

The State Sampling method is the MCS method used in this thesis work. The software produced could be extended to include the State Transition and State Duration methods. Comparing the results between the methods both in terms of computational time needed to converge on an accurate result, as well as possible differences in the results produced, could be of interest.

The work done through this thesis restricts the optimal power flow calculations to the simplified DC-method. Expanding on this to include the AC-load flow analysis could be done.

Improving the computational efficiency of the script could be advantageous. Many methods could be applied in this regard. Two examples are listed below:

- The decoupled OPF approach could reduce the time needed to compute the load flow analysis of each contingency state.
- Reduction in the sample variance could lead to the State Sampling method needing fewer years to converge.

The thesis work could also be expanded to explore the implications of multi area connections. How these composite power systems would interact when wind power is integrated could be a interesting topic to study.

References

- [1] International Renewable Energy Agency - IRENA. *Renewable Capacity Highlights*. Available at https://www.irena.org/-/media/Files/IRENA/Agency/Publication/2019/Mar/RE_capacity_highlights_2019.pdf?la=en&hash=BA9D38354390B001DC0CC9BE03EEE559C280013F (Visited at 2020/12/16).
- [2] European Environmental Agency. *Renewable energy in Europe - 2018*. Available at <https://www.eea.europa.eu/publications/renewable-energy-in-europe-2018> (Visited at 2020/12/16).
- [3] P. D. Lund et al. *Renewable and Sustainable Energy Reviews*. Available at https://econpapers.repec.org/article/eeerensus/v_3a45_3ay_3a2015_3ai_3ac_3ap_3a785-807.htm (2020/11/12).
- [4] R. Billinton and R. Mo. *Deterministic/Probabilistic Contingency Evaluation in Composite Generation and Transmission Systems, vol. 2*. IEEE Power Eng. Soc. Gen. Meet., 2004.
- [5] R. Billinton and R. N. Allan. “Power-system reliability in perspective”. In: *Electronics and Power* 30.3 (1984), pp. 231–236. DOI: 10.1049/ep.1984.0118.
- [6] Øystein Stake Laengen. “Application of Monte Carlo Simulation to Power System Adequacy Assessment”. Masters thesis. MA thesis. Norway, Trondheim, NTNU: NTNU, June 2018.
- [7] Jo Søbstad Skjævesland and Joakim Horpestad. “Quantifying the Impact of Integration Wind Power on Composite Power System Reliability”. Masters thesis. MA thesis. Norway, Trondheim, NTNU: NTNU, June 2021.
- [8] Marta Poncela Blanco et al. *Generation Adequacy methodologies review*. Tech. rep. Ispra, Italy, 2016.
- [9] P. Kundur et al. “Definition and Classification of Power System Stability”. In: *IEEE Transactions on Power Systems* 19.3 (2004), pp. 1387–1401. DOI: 10.1109/TPWRS.2004.825981.
- [10] European Commission Directorate – General for Energy. “Identification of Appropriate Generation and System Adequacy Standards for the Internal Electricity Market”. In: *European Commission* EUR 2015.1392 EN (2014). DOI: 10.2832/089498.
- [11] International Electrotechnical Commission. *Reliability*. URL: <http://www.electropedia.org/iev/iev.nsf/display?openform&ievref=>.
- [12] E. Johansson T. K. Vrana. “Overview of Power System Reliability Assessment Techniques”. In: *Cigre Colloquium Recife* (2011), pp. 1–2.
- [13] Sara Awara. “On Capacity Value of Energy-Limited Resources in Capacity Markets”. MA thesis. Calgary, Alberta: University of Calgary, Apr. 2019.

- [14] Håvard Dahl Mediaas. “Contribution of Energy Storage to Generation Adequacy Assessment”. Masters thesis. MA thesis. Norway, Trondheim, NTNU: NTNU, June 2020.
- [15] Kjetil Koldingsnes. “Reliability-based Derating Approach for Interconnectors”. Masters thesis. MA thesis. Norway, Trondheim, NTNU: NTNU, June 2017.
- [16] Abdullah M. Al-Shaalan. “Reliability Evaluation of Power Systems”. In: *Reliability and Maintenance - An Overview of Cases*. Ed. by Leo Kounis. London, UK: IntechOpen, 2020.
- [17] Ronald N. Allan Roy Billinton. *Reliability Evaluation of Power Systems*. 2nd ed. Boston, MA, United States: Springer US, 1996.
- [18] Anette Solheim. “Incorporating Demand Side Response in Power System Adequacy Studies”. Masters thesis. MA thesis. Norway, Trondheim, NTNU: NTNU, June 2019.
- [19] Mads Bjørkeland. “Generation system adequacy studies in the presence of wind energy resources”. Masters thesis. MA thesis. Norway, Trondheim, NTNU: NTNU, Feb. 2018.
- [20] NERC. *Methods to Model and Calculate Capacity Contributions of Variable Generation for Resource Adequacy Planning*. Tech. rep. Princeton, NJ, 2011.
- [21] R. Billinton and W. Li. *Reliability Assessment of Electric Power Systems Using Monte Carlo Methods*. Boston, MA: Springer, US, 1994.
- [22] Phoon Hee Yau. “Generation System Reliability Evaluations with Intermittent Renewables”. MA thesis. Glasgow, Scotland: University of Strathclyde, Sept. 2006.
- [23] Yi Luo Nian Shi. “Energy Storage System Sizing Based on a Reliability Assessment of Power Systems Integrated with Wind Power”. In: *Sustainability* 9.3 (2017). DOI: 10.1109/ITNEC.2019.8729448.
- [24] M. A. Abdullah et al. “Estimating the capacity value of energy storage integrated with wind power generation”. In: *2013 IEEE Power Energy Society General Meeting (2013)*, pp. 1–5. DOI: 10.1109/PESMG.2013.6672996.
- [25] L.L Garver. “Effective Load Carrying Capability of Generating Units”. In: *IEEE TRANSACTIONS ON POWER APPARATUS AND SYSTEMS* PAS-85.8 (1966), pp. 1–10. DOI: 10.1109/PESMG.2013.6672996.
- [26] Mikael Amelin. “Comparison of Capacity Credit Calculation Methods for Conventional Power Plants and Wind Power”. In: *IEEE TRANSACTIONS ON POWER SYSTEMS* 24.2 (2009).
- [27] A. Keane et al. “Capacity Value of Wind Power”. In: *IEEE Transactions on Power Systems* 26.2 (2011), pp. 564–572. DOI: 10.1109/TPWRS.2010.2062543.
- [28] Po Hu. “AVAILABILITY EVALUATION OF ELECTRIC POWER SYSTEMS INCLUDING WIND POWER AND ENERGY STORAGE”. PhD thesis. Saskatoon, Canada, 2009.

- [29] Ali Heshmati et al. “Wind Farm Modeling For Reliability Assessment from the Viewpoint of Interconnected Systems”. In: *Electric Power Components and Systems - ELECTR POWER COMPON SYST* 40 (Jan. 2012), pp. 257–272. DOI: 10.1080/15325008.2011.631086.
- [30] R. Billinton et al. “Adequacy Assessment Considerations in Wind Integrated Power Systems”. In: *IEEE Transactions on Power Systems* 27.4 (2012), pp. 2297–2305.
- [31] Kasper Coates et al. “Application Forms for Renewable Electricity in Developing Countries”. Trondheim, Norway: NTNU, May 2018.
- [32] S. Shi and K. L. Lo. “Reliability assessment of power system considering the impact of wind energy”. In: *IEEE Transactions on Power Systems* (2012), pp. 1–6.
- [33] Yifeng Li. “BULK SYSTEM RELIABILITY EVALUATION IN A DEREGULATED POWER INDUSTRY”. Masters thesis. MA thesis. Saskatoon, US: Department of Electrical Engineering, University of Saskatchewan, Dec. 2003.
- [34] Douglas Burden Richard. *2.1 The Bisection Algorithm”, Numerical Analysis*. 3rd ed. PWS Publishers, 1985.
- [35] C.J. Dent, A. Keane, and J.W. Bialek. “Simplified methods for renewable generation capacity credit calculation: A critical review”. In: *IEEE PES General Meeting*. 2010, pp. 1–8. DOI: 10.1109/PES.2010.5589606.
- [36] Roy Billinton et al. “Adequacy Assessment of Wind-Integrated Composite Generation and Transmission Systems”. In: *Innovations in Power Systems Reliability*. Ed. by George Anders and Alfredo Vaccaro. Springer Series in Reliability Engineering. Springer, Aug. 2011, pp. 141–167. DOI: 10.1007/978-0-85729-088-5.
- [37] Abhishek Chakraborty. *GENERATOR CAPACITY OUTAGE PROBABILITY TABLE*. Available at [https://nl.mathworks.com/matlabcentral/fileexchange/27599-generator-capacity-outage-probability-table\(2010/05/13\)](https://nl.mathworks.com/matlabcentral/fileexchange/27599-generator-capacity-outage-probability-table(2010/05/13)).
- [38] R. N. Allan et al. “A reliability test system for educational purposes-basic distribution system data and results”. In: *IEEE Transactions on Power Systems* 6.2 (1991), pp. 813–820. DOI: 10.1109/59.76730.
- [39] R. Billinton and S. Jonnavithula. “A test system for teaching overall power system reliability assessment”. In: *IEEE Transactions on Power Systems* 11 (1996), pp. 1670–1676.
- [40] R. Billinton et al. “A Reliability Test System for Educational Purposes-Basic Data”. In: *IEEE Power Engineering Review* 9.8 (1989), pp. 67–68. DOI: 10.1109/MPER.1989.4310918.
- [41] C. Barrows et al. “The IEEE reliability test system: A proposed 2019 Update”. In: *IEEE Transactions on Power Systems* 35 (2019), pp. 119–127.

- [42] J. M. Morales C. Ordoudis P. Pinson and M. Zugno. “An updated version of the IEEE RTS 24-bus system for electricity market and power system operation studies”. In: *Technical University of Denmark* (2016), pp. 0885–8950.
- [43] C. Grigg et al. “The IEEE reliability test system-1996. A report prepared by the reliability test system task force of the application of probability methods subcommittee”. In: *IEEE Transactions on power systems* 14 (1996), pp. 1010–1020.

A COPT Example Code

The source code is collected in the forum of MathWorks, written by Abhishek Chakraborty [37].

```
% This is a function file: GeneratorCOPTG,PR,A
% This calculates the 'Outage Probability' for a single Power SGeneratorCOPTMatrixion
% G stands for number of generating unit
% PR stands for Power Ratings of each unit in Array form
% A stands for Availability of each unit in Array form

function Generator_COPTG,PR,A
format short g
X=ff2nG;
InitiationMatrix=[zeros1,2^G;zeros1,2^G;ones1,2^G;zeros1,2^G];
GeneratorCOPTMatrixTemp=InitiationMatrix';
for j=1:2^G
for i=1:G
    if Xj,i==0
        GeneratorCOPTMatrixTempj,1=GeneratorCOPTMatrixTempj,1+PRi,1;
        GeneratorCOPTMatrixTempj,3=GeneratorCOPTMatrixTempj,3+Ai,1;
    else
        GeneratorCOPTMatrixTempj,2=GeneratorCOPTMatrixTempj,2+PRi,1;
        GeneratorCOPTMatrixTempj,3=GeneratorCOPTMatrixTempj,3+1-Ai,1;
    end
end
end
end
TemporaryMatrix=GeneratorCOPTMatrixTemp;
for m=1:2^G
    for n=1:2^G
        ifGeneratorCOPTMatrixTempm,1==GeneratorCOPTMatrixTempn,1&& m~=n && n>m
            GeneratorCOPTMatrixTempm,3=GeneratorCOPTMatrixTempn,3+GeneratorCOPTMatrixTempn,3;
        else end
    end
end
for m=1:2^G
    for n=1:2^G
        ifGeneratorCOPTMatrixTempm,1==GeneratorCOPTMatrixTempn,1 && m<n && m~=n && GeneratorCOPTMatrixTempm,1~=0
            GeneratorCOPTMatrixTempn,:=zeros;
        else end
    end
end
for m=1:1:2^G-1
    for n=1:1:2^G-1
        if GeneratorCOPTMatrixTempn,1<GeneratorCOPTMatrixTempn+1,1
            temp1=GeneratorCOPTMatrixTempn,1;
            temp2=GeneratorCOPTMatrixTempn,2;
```


B MCS Example codes

B.1 Example State Duration

```
function [States_comp1,States_comp2,TimeStateChange,PowerOutput] = ExampleStateDuration

%Simple example code for demonstration of MCS State Duration Method
%System of two generators comp1 & comp2, different failure rates and
%power output.
%Not in any way optimized or general, but works on a small scale on this specific system

P_comp1 = 15; % MW,
P_comp2 = 20; % MW

FR_RR_comp1 = 0.25; %Failure Rate and Repair Rate
FR_RR_comp2 = 0.20; %Failure Rate and Repair Rate

scope = 25; % Number of time steps

%Initializing values for collection of data
States_comp1 = 0;
States_comp2 = 0;
TimeStateChange = 0;

i = 0;
counter = 1;

while i < scope
    R_comp1 = rand; %Random number in range 0,1
    R_comp2 = rand;
    T_comp1 = - 1/FR_RR_comp1 * logR_comp1; % Sampling of value of state duration
    T_comp2 = - 1/FR_RR_comp2 * logR_comp2;
    if i + ceilT_comp1 > scope && i + ceilT_comp2 > scope
        break
    end
    if T_comp1 < T_comp2
        i = i + ceilT_comp1;
        counter = counter + 1;
        TimeStateChangecounter = i;
        if States_comp1counter-1 == 0
            States_comp1counter = 1;
            States_comp2counter = States_comp2counter-1;
        else
            States_comp1counter = 0;
            States_comp2counter = States_comp2counter-1;
        end
    end
end
```

```

        end
    else
        i = i + ceilT_comp2;
        counter = counter + 1;
        TimeStateChangecounter = i;
        if States_comp2counter-1 == 0
            States_comp2counter = 1;
            States_comp1counter = States_comp1counter-1;
        else
            States_comp2counter = 0;
            States_comp1counter = States_comp1counter-1;
        end
    end
end
end

n = 0;
while n < lengthTimeStateChange % Calculating power at times of state change
    n = n + 1;
    PowerOutputn = 1 - States_comp1n * P_comp1 + 1 - States_comp2n * P_comp2;
end
end

```

B.2 Example State Transition

```
function [States_comp1,States_comp2,TimeStateChange,PowerOutput] = ExampleStateTransition

%Simple example code for demonstration of MCS State Transition Method
%System of two generators comp1 & comp2, different failure rates and
%power output.
%Not in any way optimized or general, but works on a small scale on this specific system

P_comp1 = 15; % MW,
P_comp2 = 20; % MW

FR_RR_comp1 = 0.25; %Failure Rate and Repair Rate
FR_RR_comp2 = 0.20; %Failure Rate and Repair Rate

U_tot = FR_RR_comp1 + FR_RR_comp2;
U_comp1 = FR_RR_comp1 / FR_RR_comp1 + FR_RR_comp2; %State probability of change in comp 1
%Since there are only two components, we only need the one.

scope = 25; % Number of time steps

%Initializing values for collection of data
States_comp1 = 0;
States_comp2 = 0;
TimeStateChange = 0;

i = 0;
counter = 1;

while i < scope
    U_1 = rand;
    U_2 = rand;
    T = - 1/U_tot * log(U_2);
    counter = counter + 1;
    i = i + ceil(T);
    if i > scope
        break
    end
    TimeStateChangecounter = i;
    if U_1 < U_comp1
        if States_comp1counter-1 == 0
            States_comp1counter = 1;
            States_comp2counter = States_comp2counter-1;
        else
            States_comp1counter = 0;
            States_comp2counter = States_comp2counter-1;
        end
    end
end
else
```

```
    if States_comp2counter-1 == 0
        States_comp2counter = 1;
        States_comp1counter = States_comp1counter-1;
    else
        States_comp2counter = 0;
        States_comp1counter = States_comp1counter-1;
    end
end
end

n = 0;
while n < lengthTimeStateChange % Calculating power at times of state change
    n = n + 1;
    PowerOutputn = 1 - States_comp1n * P_comp1 + 1 - States_comp2n * P_comp2;
end
end
```

C RBTS

The RBTS (Roy Billinton Test System) is a 6-bus composite system including 9 power transmission lines. It was developed at the University of Saskatchewan in Canada for education and small scale PSR testing. It aims to be sufficiently simple enough to be able to be subject to a large number of different PSR studies without increasing the time of simulations or hand calculations unnecessary. It also aims to be sufficiently detailed to model the nuances associated with PSR [38]. The system is given sufficient parameters to be viable for both HL-I and HL-II studies. [39]

The generation system consists of 11 generators; 4 thermal generators at bus 1 and 7 hydro generators at bus 2 [40]. The total generation capacity of the system is 240 MW and a peak load of 185 MW. RBTS connections and the peak load of the different buses are shown in Figure C.1.1. The data necessary to preform HL-II studies can be found in tables C.2.1, C.3.2, C.3.1 and C.4.1.

C.1 RBTS Topology, single line diagram

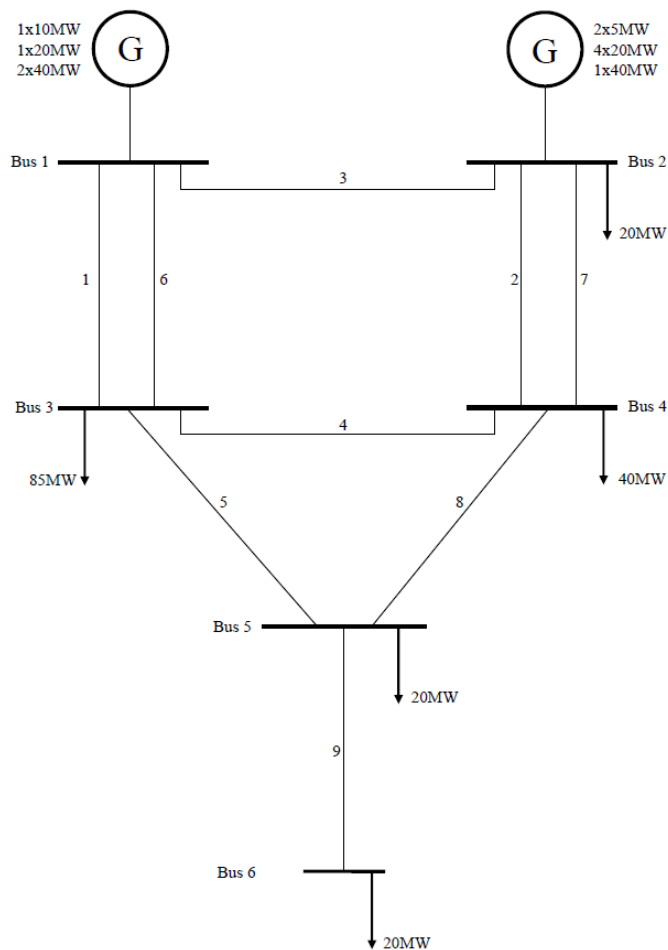


Figure C.1.1: Single line diagram of the Roy Billinton Test System

C.2 RBTS Generator data

Table C.2.1: RBTS generator data

Generator	Capacity [MW]	Bus	Reactive min [MVar]	Reactive max [MVar]	FOR	Failure rate [1/year]	Repair rate [1/year]
1	10	1	0	7	0.020	4.0	196.0
2	20	1	-7	12	0.025	5.0	195.0
3	40	1	-15	17	0.030	6.0	194.0
4	40	1	-15	17	0.030	6.0	194.0
5	5	2	0	5	0.010	2.0	198.0
6	5	2	0	5	0.010	2.0	198.0
7	20	2	-7	12	0.015	2.4	157.6
8	20	2	-7	12	0.015	2.4	157.6
9	20	2	-7	12	0.015	2.4	157.6
10	20	2	-7	12	0.015	2.4	157.6
11	40	2	-15	17	0.020	3.0	147.0

C.3 RBTS Network data

Table C.3.1: RBTS network parameters

Line	From Bus	To Bus	Resistance [pu]	Reactance [pu]	X	B/2 [pu]	Current Rating [pu]
1	1	3	0.0342	0.18		0.0106	0.85
2	2	4	0.114	0.6		0.0352	0.71
3	1	2	0.0912	0.48		0.0282	0.71
4	3	4	0.0228	0.12		0.0071	0.71
5	3	5	0.0228	0.12		0.0071	0.71
6	1	3	0.0342	0.18		0.0106	0.85
7	2	4	0.114	0.6		0.0352	0.71
8	4	5	0.0228	0.12		0.0071	0.71
9	5	6	0.0228	0.12		0.0071	0.71

Table C.3.2: RBTS outage data

Line	From Bus	To Bus	Failure rate [1/year]	MTTR [hours]	FOR
1	1	3	1.5	10	0.00171
2	2	4	5.0	10	0.00568
3	1	2	4.0	10	0.00455
4	3	4	1.0	10	0.00114
5	3	5	1.0	10	0.00114
6	1	3	1.5	10	0.00171
7	2	4	5.0	10	0.00568
8	4	5	1.0	10	0.00114
9	5	6	1.0	10	0.00114

C.4 RBTS Bus data

Table C.4.1: RBTS Bus data

Bus	Share of load	Vmin [p.u]	Vmax [p.u]	Curtailement cost [\$/kWh]
1	0	0.97	1.05	0
2	0.1081	0.97	1.05	9.6325
3	0.4595	0.97	1.05	4.3769
4	0.2162	0.97	1.05	8.0267
5	0.1081	0.97	1.05	8.6323
6	0.1081	0.97	1.05	5.5132

D IEEE-RTS

The IEEE-RTS is a widely known and used test system. First developed in 1979, it has later been modified into multiple different versions [41, 42]. The following information presents the 1996 version (IEEE-RTS96).

The IEEE-RTS exist in three configurations. The 24-bus system, the two-area 48-bus system, and the three-area 73-bus system [43, 7]. The 24-bus system is the configuration used in this thesis, illustrated in Figure D.1.1.

The IEEE-RTS is more complex than the RBTS, with the 24-bus system including 32 generators with a generation capacity ranging from 12 MW to 400 MW. The maximum generation capacity of the system is 3405 MW and it's peak load is 2850 MW. The system is designed to be nuanced enough be preformed both HL-I and HL-II studies on [41]. The system data needed for an HL-II study is given in tables D.2.1, D.3.2, D.3.1 and D.4.1.

D.1 RTS Topology, single line diagram

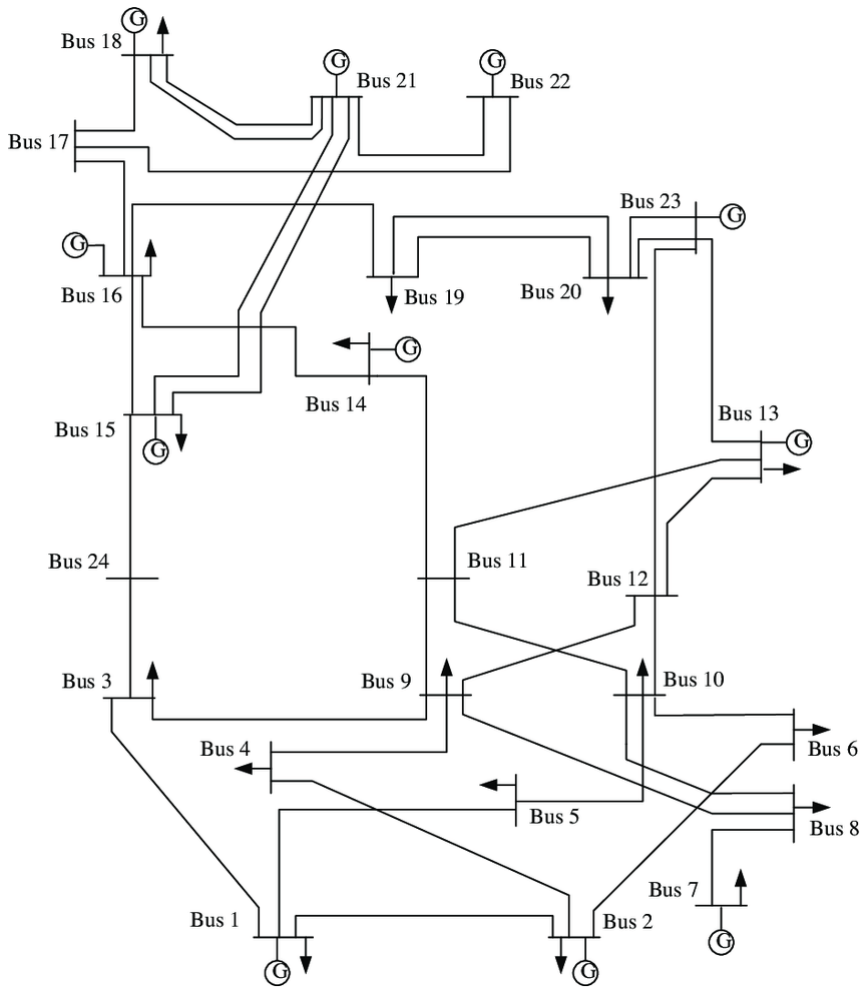


Figure D.1.1: Single line diagram of the IEEE-RTS

D.2 RTS Generator data

Table D.2.1: RTS generator data

Capacity [MW]	Bus	X_{min} [MVar]	X_{max} [MVar]	FOR	MTTF	MTTR
12	15	0	6	0.02	2940	60
12	15	0	6	0.02	2940	60
12	15	0	6	0.02	2940	60
12	15	0	6	0.02	2940	60
12	15	0	6	0.02	2940	60
20	1	0	10	0.1	450	50
20	1	0	10	0.1	450	50
20	2	0	10	0.1	450	50
20	2	0	10	0.1	450	50
50	22	-10	16	0.01	1980	20
50	22	-10	16	0.01	1980	20
50	22	-10	16	0.01	1980	20
50	22	-10	16	0.01	1980	20
50	22	-10	16	0.01	1980	20
50	22	-10	16	0.01	1980	20
76	1	-25	30	0.02	1960	40
76	1	-25	30	0.02	1960	40
76	2	-25	30	0.02	1960	40
76	2	-25	30	0.02	1960	40
100	7	0	60	0.04	1200	50
100	7	0	60	0.04	1200	50
100	7	0	60	0.04	1200	50
155	15	-50	80	0.04	960	40
155	16	-50	80	0.04	960	40
155	23	-50	80	0.04	960	40
155	23	-50	80	0.04	960	40
197	13	0	80	0.05	950	50
197	13	0	80	0.05	950	50
197	13	0	80	0.05	950	50
350	23	-25	150	0.08	1150	100
400	18	-50	200	0.12	1100	150
400	21	-50	200	0.12	1100	150
0	14	-50	200	0	-	-
0	6	-100	0	0	-	-

D.3 RTS Network data

Table D.3.1: RTS network parameters

Line	From Bus	To Bus	Resistance [pu]	Reactance [pu]	X	B/2 [pu]	Current Rating [pu]
1	1	2	0.0026	0.0139		0.23055	1.93
2	1	3	0.0546	0.2112		0.0286	2.08
3	1	5	0.0218	0.0845		0.01145	2.08
4	2	4	0.0328	0.1267		0.01715	2.08
5	2	6	0.0497	0.192		0.026	2.08
6	3	9	0.0308	0.119		0.0161	2.08
7	3	24	0.0023	0.0839		0	5.1
8	4	9	0.0268	0.1037		0.01405	2.08
9	5	10	0.0228	0.0883		0.01195	2.08
10	6	10	0.0139	0.0605		1.2295	1.93
11	7	8	0.0159	0.0614		0.0083	2.08
12	8	9	0.0427	0.1651		0.02235	2.08
13	8	10	0.0427	0.1651		0.02235	2.08
14	9	11	0.0023	0.0839		0	5.1
15	9	12	0.0023	0.0839		0	5.1
16	10	11	0.0023	0.0839		0	5.1
17	10	12	0.0023	0.0839		0	5.1
18	11	13	0.0061	0.0476		0.04995	6
19	11	14	0.0054	0.0418		0.04395	6
20	12	13	0.0061	0.0476		0.04995	6
21	12	23	0.0124	0.0966		0.1015	6
22	13	23	0.0111	0.0865		0.0909	6
23	14	16	0.005	0.0389		0.0409	6
24	15	16	0.0022	0.0173		0.0182	6
25	15	21	0.0063	0.049		0.0515	6
26	15	21	0.0063	0.049		0.0515	6
27	15	24	0.0067	0.0519		0.05455	6
28	16	17	0.0033	0.0259		0.02725	6
29	16	19	0.003	0.0231		0.02425	6
30	17	18	0.0018	0.0144		0.01515	6
31	17	22	0.0135	0.1053		0.1106	6
32	18	21	0.0033	0.0259		0.02725	6
33	18	21	0.0033	0.0259		0.02725	6
34	19	20	0.0051	0.0396		0.04165	6
35	19	20	0.0051	0.0396		0.04165	6
36	20	23	0.0028	0.0216		0.02275	6
37	20	23	0.0028	0.0216		0.02275	6
38	21	22	0.0087	0.0678		0.0712	6

Table D.3.2: RTS outage data

Line	From Bus	To Bus	Failure rate [1/year]	MTTR [hours]	FOR
1	1	2	0.24	16	0.000438164
2	1	3	0.51	10	0.000581853
3	1	5	0.33	10	0.000376570
4	2	4	0.39	10	0.000445007
5	2	6	0.48	10	0.000547645
6	3	9	0.38	10	0.000433602
7	3	24	0.02	768	0.001750356
8	4	9	0.36	10	0.000410790
9	5	10	0.34	10	0.000387977
10	6	10	0.33	35	0.001316757
11	7	8	0.30	10	0.000342349
12	8	9	0.44	10	0.000502031
13	8	10	0.44	10	0.000502031
14	9	11	0.02	768	0.001750356
15	9	12	0.02	768	0.001750356
16	10	11	0.02	768	0.001750356
17	10	12	0.02	768	0.001750356
18	11	13	0.40	11	0.000502031
19	11	14	0.39	11	0.000489486
20	12	13	0.40	11	0.000502031
21	12	23	0.52	11	0.000652542
22	13	23	0.49	11	0.000614918
23	14	16	0.38	11	0.000476941
24	15	16	0.33	11	0.000414212
25	15	21	0.41	11	0.000514575
26	15	21	0.41	11	0.000514575
27	15	24	0.41	11	0.000514575
28	16	17	0.35	11	0.000439305
29	16	19	0.34	11	0.000426758
30	17	18	0.32	11	0.000401665
31	17	22	0.54	11	0.000677623
32	18	21	0.35	11	0.000439305
33	18	21	0.35	11	0.000439305
34	19	20	0.38	11	0.000476941
35	19	20	0.38	11	0.000476941
36	20	23	0.34	11	0.000426758
37	20	23	0.34	11	0.000426758
38	21	22	0.45	11	0.000564749

D.4 RTS Bus data

Table D.4.1: RTS Bus data

Bus	Share of load	Vmin [p.u]	Vmax [p.u]	Curtailement cost [\$/kWh]
1	0.038	0.95	1.05	8.981
2	0.034	0.95	1.05	7.3606
3	0.063	0.95	1.05	5.8990
4	0.026	0.95	1.05	9.5992
5	0.025	0.95	1.05	9.2323
6	0.048	0.95	1.05	6.5238
7	0.044	0.95	1.05	7.0291
8	0.06	0.95	1.05	7.7742
9	0.061	0.95	1.05	3.6623
10	0.068	0.95	1.05	5.1940
11	0	0.95	1.05	0.0000
12	0	0.95	1.05	0.0000
13	0.093	0.95	1.05	7.2813
14	0.068	0.95	1.05	4.3717
15	0.111	0.95	1.05	5.9744
16	0.035	0.95	1.05	7.2305
17	0	0.95	1.05	0.0000
18	0.117	0.95	1.05	5.6149
19	0.064	0.95	1.05	4.5430
20	0.045	0.95	1.05	5.6836
21	0	0.95	1.05	0.0000
22	0	0.95	1.05	0.0000
23	0	0.95	1.05	0.0000
24	0	0.95	1.05	0.0000

E Individual bus reliability indices and standard deviation when ELCC is based on LOLE

E.1 RBTS

Table E.1.1: The individual bus indices for the RBTS, when ELCC is produced with LOLE as the basis. These results are a product of the RBTS analysis performed in Chapter 4.2.1. These are the indices of the new system, not including the benchmark system. "std" refers to the standard deviation.

Bus	LOLE	std	LOLP	EENS	std
1	0.0000	0.0000	0.000000	0.0000	0.0000
2	0.0010	0.0316	0.000000	0.0147	0.4809
3	1.2127	1.1044	0.000139	11.0318	13.8778
4	0.0000	0.0000	0.000000	0.0000	0.0000
5	0.0115	0.1066	0.000001	0.1507	1.4237
6	9.9742	3.0662	0.001142	129.3046	40.7251

E.2 MRBTS

Table E.2.1: The individual bus indices for the MRBTS, when ELCC is produced with LOLE as the basis. These results are a product of the MRBTS analysis performed in Chapter 4.2.2. These are the indices of the new system, not including the benchmark system. "std" refers to the standard deviation.

Bus	LOLE	std	LOLP	EENS	std
1	0.0000	0.0000	0.000000	0.0000	0.0000
2	0.0003	0.0158	0.000000	0.0023	0.1465
3	1.1093	1.0546	0.000127	9.7561	13.1630
4	0.0000	0.0000	0.000000	0.0000	0.0000
5	0.0097	0.0983	0.000001	0.1291	1.3277
6	0.0192	0.1374	0.000002	0.2482	1.8155

E.3 RTS

Table E.3.1: The individual bus indices for the RTS, when ELCC is produced with LOLE as the basis. These results are a product of the RTS analysis performed in Chapter 4.2.3. These are the indices of the new system, not including the benchmark system. "std" refers to the standard deviation.

Bus	LOLE	std	LOLP	EENS	std
1	0.0000	0.0000	0.000000	0.0000	0.0000
2	0.0000	0.0000	0.000000	0.0000	0.0000
3	0.0000	0.0000	0.000000	0.0000	0.0000
4	0.0005	0.0224	0.000000	0.0215	0.9768
5	0.0018	0.0418	0.000000	0.0834	2.0268
6	0.0067	0.0819	0.000001	0.5925	7.3050
7	2.9333	1.7063	0.000336	226.7297	135.4432
8	0.0020	0.0447	0.000000	0.2255	5.1356
9	9.4757	3.0664	0.001085	856.2559	321.9429
10	0.1200	0.3473	0.000014	8.9761	32.1690
11	0.0000	0.0000	0.000000	0.0000	0.0000
12	0.0000	0.0000	0.000000	0.0000	0.0000
13	0.0000	0.0000	0.000000	0.0000	0.0000
14	2.8430	1.6479	0.000325	258.4288	181.5785
15	0.0000	0.0000	0.000000	0.0000	0.0000
16	0.0000	0.0000	0.000000	0.0000	0.0000
17	0.0000	0.0000	0.000000	0.0000	0.0000
18	0.0135	0.1154	0.000002	1.0609	11.6445
19	0.6188	0.7727	0.000071	50.0775	78.1182
20	0.0000	0.0000	0.000000	0.0000	0.0000
21	0.0000	0.0000	0.000000	0.0000	0.0000
22	0.0000	0.0000	0.000000	0.0000	0.0000
23	0.0000	0.0000	0.000000	0.0000	0.0000
24	0.0000	0.0000	0.000000	0.0000	0.0000

F Individual bus reliability indices and standard deviation when ELCC is based on EENS

F.1 RBTS

Table F.1.1: The individual bus indices for the RBTS, when ELCC is produced with EENS as the basis. These results are a product of the RBTS analysis performed in Chapter 4.3.1. These are the indices of the new system, not including the benchmark system. "std" refers to the standard deviation.

Bus	LOLE	std	LOLP	EENS	std
1	0.0000	0.0000	0.000000	0.0000	0.0000
2	0.0015	0.0387	0.000000	0.0157	0.4177
3	0.8333	0.9185	0.000095	7.5989	11.4253
4	0.0000	0.0000	0.000000	0.0000	0.0000
5	0.0135	0.1154	0.000002	0.1622	1.4273
6	9.9543	3.1028	0.001139	124.8504	40.0603

F.2 MRBTS

Table F.2.1: The individual bus indices for the MRBTS, when ELCC is produced with EENS as the basis. These results are a product of the MRBTS analysis performed in Chapter 4.3.2. These are the indices of the new system, not including the benchmark system. "std" refers to the standard deviation.

Bus	LOLE	std	LOLP	EENS	std
1	0.0000	0.0000	0.000000	0.0000	0.0000
2	0.0010	0.0316	0.000000	0.0155	0.4976
3	1.1247	1.0554	0.000129	10.1729	13.4563
4	0.0003	0.0158	0.000000	0.0089	0.5656
5	0.0143	0.1185	0.000002	0.1894	1.6117
6	0.0260	0.1638	0.000003	0.3448	2.2246

F.3 RTS

Table F.3.1: The individual bus indices for the RTS, when ELCC is produced with EENS as the basis. These results are a product of the RTS analysis performed in Chapter 4.3.3. These are the indices of the new system, not including the benchmark system. "std" refers to the standard deviation.

Bus	LOLE	std	LOLP	EENS	std
1	0.0000	0.0000	0.000000	0.0000	0.0000
2	0.0000	0.0000	0.000000	0.0000	0.0000
3	0.0000	0.0000	0.000000	0.0000	0.0000
4	0.0010	0.0316	0.000000	0.0546	1.7703
5	0.0015	0.0387	0.000000	0.0531	1.3914
6	0.0043	0.0651	0.000000	0.3759	5.8768
7	2.9688	1.7229	0.000340	229.6085	136.8322
8	0.0020	0.0447	0.000000	0.1717	3.9414
9	9.6137	3.0825	0.001100	874.8275	327.2723
10	0.1222	0.3498	0.000014	8.9047	32.0903
11	0.0000	0.0000	0.000000	0.0000	0.0000
12	0.0000	0.0000	0.000000	0.0000	0.0000
13	0.0000	0.0000	0.000000	0.0000	0.0000
14	2.8810	1.7136	0.000330	259.9848	188.3649
15	0.0000	0.0000	0.000000	0.0000	0.0000
16	0.0000	0.0000	0.000000	0.0000	0.0000
17	0.0000	0.0000	0.000000	0.0000	0.0000
18	0.0143	0.1185	0.000002	0.9189	11.2887
19	0.6350	0.8040	0.000073	51.7963	79.9574
20	0.0003	0.0158	0.000000	0.0056	0.3516
21	0.0000	0.0000	0.000000	0.0000	0.0000
22	0.0000	0.0000	0.000000	0.0000	0.0000
23	0.0000	0.0000	0.000000	0.0000	0.0000
24	0.0000	0.0000	0.000000	0.0000	0.0000

G Coefficients of variation for individual buses when ELCC is based on LOLE

G.1 RBTS

Table G.1.1: The coefficient of variation for the different buses when ELCC is produced with LOLE as the basis. Resulting from the RBTS analysis performed in Chapter 4.2.1. BM refers to the benchmark system, NS refers to the new system where wind power generation is integrated and the load is increased.

Bus	$LOLE_{BM}$	$EENS_{BM}$	$LOLE_{NS}$	$EENS_{NS}$
1	NaN	NaN	NaN	NaN
2	0.3777	0.3929	0.4998	0.3929
3	0.0145	0.0203	0.0144	0.0203
4	0.7070	0.7074	NaN	0.7074
5	0.1365	0.1395	0.1466	0.1395
6	0.0050	0.0052	0.0049	0.0052
Total	0.0047	0.0050	0.0046	0.0048

G.2 MRBTS

Table G.2.1: The coefficient of variation for the different buses when ELCC is produced with LOLE as the basis. Resulting from the MRBTS analysis performed in Chapter 4.2.2. BM refers to the benchmark system, NS refers to the new system where wind power generation is integrated and the load is increased.

Bus	$LOLE_{BM}$	$EENS_{BM}$	$LOLE_{NS}$	$EENS_{NS}$
1	NaN	NaN	NaN	NaN
2	0.4470	0.4559	1.0000	0.4559
3	0.0148	0.0201	0.0150	0.0201
4	NaN	NaN	NaN	NaN
5	0.1554	0.1603	0.1594	0.1603
6	0.1008	0.1040	0.1129	0.1040
Total	0.0146	0.0197	0.0149	0.0211

G.3 RTS

Table G.3.1: The coefficient of variation for the different buses when ELCC is produced with LOLE as the basis. Resulting from the RTS analysis performed in Chapter 4.2.3. BM refers to the benchmark system, NS refers to the new system where wind power generation is integrated and the load is increased.

Bus	$LOLE_{BM}$	$EENS_{BM}$	$LOLE_{NS}$	$EENS_{NS}$
1	NaN	NaN	NaN	NaN
2	NaN	NaN	NaN	NaN
3	NaN	NaN	NaN	NaN
4	0.3011	0.3104	0.7070	0.3104
5	0.3777	0.3837	0.3777	0.3837
6	0.1883	0.1924	0.1918	0.1924
7	0.0091	0.0093	0.0092	0.0093
8	0.4998	0.5164	0.3532	0.5164
9	0.0051	0.0059	0.0051	0.0059
10	0.0451	0.0561	0.0458	0.0561
11	NaN	NaN	NaN	NaN
12	NaN	NaN	NaN	NaN
13	NaN	NaN	NaN	NaN
14	0.0092	0.0112	0.0092	0.0112
15	NaN	NaN	NaN	NaN
16	NaN	NaN	NaN	NaN
17	NaN	NaN	NaN	NaN
18	0.1221	0.1553	0.1352	0.1553
19	0.0198	0.0239	0.0197	0.0239
20	NaN	NaN	NaN	NaN
21	NaN	NaN	NaN	NaN
22	NaN	NaN	NaN	NaN
23	NaN	NaN	NaN	NaN
24	NaN	NaN	NaN	NaN
Total	0.0044	0.0060	0.0045	0.0060

H Coefficients of variation for individual buses when ELCC is based on EENS

H.1 RBTS

Table H.1.1: The coefficient of variation for the different buses when ELCC is produced with EENS as the basis. Resulting from the RBTS analysis performed in Chapter 4.3.1. BM refers to the benchmark system, NS refers to the new system where wind power generation is integrated and the load is increased.

Bus	$LOLE_{BM}$	$EENS_{BM}$	$LOLE_{NS}$	$EENS_{NS}$
1	NaN	NaN	NaN	NaN
2	0.4080	0.4139	0.4080	0.4139
3	0.0147	0.0203	0.0174	0.0203
4	NaN	NaN	NaN	NaN
5	0.1482	0.1517	0.1352	0.1517
6	0.0050	0.0052	0.0049	0.0052
Total	0.0048	0.0050	0.0047	0.0050

H.2 MRBTS

Table H.2.1: The coefficient of variation for the different buses when ELCC is produced with EENS as the basis. Resulting from the MRBTS analysis performed in Chapter 4.3.2. BM refers to the benchmark system, NS refers to the new system where wind power generation is integrated and the load is increased.

Bus	$LOLE_{BM}$	$EENS_{BM}$	$LOLE_{NS}$	$EENS_{NS}$
1	NaN	NaN	NaN	NaN
2	0.3330	0.3459	0.4998	0.3459
3	0.0148	0.0208	0.0148	0.0208
4	0.7070	0.7071	1.0000	0.7071
5	0.1637	0.1685	0.1315	0.1685
6	0.1093	0.1128	0.0996	0.1128
Total	0.0146	0.0205	0.0147	0.0206

H.3 RTS

Table H.3.1: The coefficient of variation for the different buses when ELCC is produced with EENS as the basis. Resulting from the RTS analysis performed in Chapter 4.3.3. BM refers to the benchmark system, NS refers to the new system where wind power generation is integrated and the load is increased.

Bus	$LOLE_{BM}$	$EENS_{BM}$	$LOLE_{NS}$	$EENS_{NS}$
1	NaN	NaN	NaN	NaN
2	NaN	NaN	NaN	NaN
3	NaN	NaN	NaN	NaN
4	0.7070	0.7074	0.4998	0.7074
5	0.3777	0.3872	0.4080	0.3872
6	0.1883	0.1946	0.2420	0.1946
7	0.0091	0.0094	0.0092	0.0094
8	0.2883	0.2927	0.3532	0.2927
9	0.0050	0.0059	0.0051	0.0059
10	0.0441	0.0555	0.0452	0.0555
11	NaN	NaN	NaN	NaN
12	NaN	NaN	NaN	NaN
13	NaN	NaN	NaN	NaN
14	0.0092	0.0109	0.0094	0.0109
15	NaN	NaN	NaN	NaN
16	NaN	NaN	NaN	NaN
17	NaN	NaN	NaN	NaN
18	0.1260	0.1658	0.1315	0.1658
19	0.0195	0.0238	0.0200	0.0238
20	NaN	NaN	1.0000	NaN
21	NaN	NaN	NaN	NaN
22	NaN	NaN	NaN	NaN
23	NaN	NaN	NaN	NaN
24	NaN	NaN	NaN	NaN
Total	0.0044	0.0059	0.0045	0.0061

I Matlab Script

Restricted public access

